Plant selection and ecological microhabitat drive domestications of shrub-associated microbiomes in a revegetated shrub ecosystem

Zongrui Lai[1]*, Yanfei Sun[2], Yang Yu[1], Zhen Liu[3], Yuxuan Bai[1], Yangui Qiao[1], Lin Miao[1], Weiwei She[1], Shugao Qin[1], Wei Feng[1]

[1]Yanchi Research Station, School of Soil and Water Conservation, Beijing Forestry University, Beijing 100083, China

[2]Key Laboratory of Genetics and Germplasm Innovation of Tropical Special Forest Trees and Ornamental Plants, Ministry of Education, College of Forestry, Hainan University, Haikou, 570228, China

[3]CAS Engineering Laboratory for Yellow River Delta Modern Agriculture, Institute of Geographic Sciences and Natural Resources Research, Chinese Academy of Sciences, Beijing, 100101, China

Corresponding Author:

Zongrui Lai

Institute: School of Soil and Water Conservation, Beijing Forestry University.

Address: No. 35 Qinghua Eastroad, School of Soil and Water Conservation, Beijing Forestry University, Haidian District, Beijing 100083, P. R. China

Tel: +86 10 62336608 (Zongrui Lai)

Fax: +86 10 62336172

E-mail: laizr.602@gmail.com

Abstract

Shrubs are used for revegetation of degraded dryland ecosystem worldwide and could recruit large numbers of microbes from the soil; however, the plant-associated microbiome assembly and the effect of plant introduction on the soil microbiomes are not fully understood. We detected shrub-associated microbes from five ecological microhabitats, including the leaves, litter, roots, rhizosphere, and root zone, across four xeric shrub plantations (*Artemisia ordosica*, *Caragana korshinskii*, *Hedysarum mongolicum*, and *Salix psammophila*). To detect the patterns of shrub-associated microbiome assembly, 16S and ITS2 rRNA gene sequencing was performed. PERMANOVA and differential abundance analysis demonstrated that changes in the bacterial and fungal communities were more dependent on the microhabitats rather than on the plant species, with distinct niche differentiation. Moreover, source tracking and nestedness analysis showed that shrub-associated bacteria were primarily derived from bulk soils and slightly pruned in different microhabitats; however, a similar pattern was not found for fungi. Furthermore, the surrounding zone of roots was a hotpot for microbial recruitments of revegetated shrubs. Null model analysis indicated that homogeneous selection of determinism dominated the bacterial communities, whereas dispersal limitation and undominated process of stochasticity drove the assembly of fungal communities. Our findings indicate that ecological microhabitat of revegetated shrublands was the main predictor of the bacterial and fungal compositional variances. This study will help advance our understanding of the mechanism underlying the plant-soil microbiome feedbacks during the initial plant-establishment period in a dryland ecosystem. Further, this work provides theoretical reference for establishment and sustainable management of shrublands in drylands.

Keywords: dryland ecosystem, plant microbiomes, community assembly, plant-microbe interactions,

co-occurrence networks

1. Introduction

Shrubs are foundation species in fragile dryland ecosystems and performs diverse ecological functions, such as maintaining species diversity, controlling soil erosion, and promoting soil formation (Maestre et al., 2021). Each plant taxon harbours a characteristic mixture of microorganisms, collectively termed as the 'plant microbiota' (Xu et al., 2021; Vandenkoornhuyse et al., 2015). These plant-specific microbiomes impact the nutrition and water acquisition of xeric plants, suppress diseases, and support plant health and resistance to harsh environments (i.e., drought, salt, and high temperature) (Cordovez et al., 2019; Trivedi et al., 2020); thereby, driving plant-soil feedbacks (Delgado-Baquerizo et al., 2020). Drylands, covering approximately 40% of the Earth's land surface, are expanding globally due to climate warming (Berg and McColl, 2021) and contain ubiquitous microbial species (Soussi et al., 2016). Many studies have focused on certain traits of soil microbes in drylands, such as the diversity, phyletic classification, and biogeography (Maestre et al., 2015; Soussi et al., 2016; Sun et al., 2020); however, the interplay between desert plants and soil microbiomes remains largely elusive, which limits the understanding of plant-soil feedback. Further, an improved understanding of the plant-soil microbiomes can improve degraded land restoration programs and increase the productivity of desert ecosystems in the future (Trivedi et al., 2019).

Although the soil microbiome is a common reservoir of microbes, plants (i.e., leaves, stem, and roots) provide diverse microhabitats for colonization by numerous microorganisms (Beckers et al., 2017). Plant-associated microbiomes acting as a second genome has received substantial attention in the recent years (Berg et al., 2014; Turner et al., 2013). Several studies have demonstrated that plant-associated microbial composition and functions are regulated by plant host genotype (Beckers et al., 2017; Soussi

et al., 2016; Vandenkoornhuyse et al., 2015), i.e., each plant habitat harbours its own characteristic microbiome (Cordovez et al., 2019). Moreover, host plants can provide a number of habitats for microorganisms and then subtly affect microbiomes that confer tolerance to abiotic stress by supplying photosynthetic carbon (Müller et al., 2016; Xu et al., 2021). For example, root exudate and rhizodeposition predominantly influence the rhizosphere microbiota (Gupta et al., 2021; Zhalnina et al., 2018). In the phyllosphere, cytokinins drive the assembly and function of microbiomes (Hu et al., 2018). Recent studies indicate that plant microbiome assembly and function are profoundly affected by different seasons or plant developmental stages (Xiong et al., 2021a; Aleklett et al., 2022). In drylands, plants thrive under prolonged environmental stresses, such as high irradiance, drought, and salt accumulation, through the development of specific physiological and molecular extremophile traits (VanWallendael et al., 2019; Van Zelm et al., 2020). Previous studies have shown that large plant microbiomes, special root-associated bacteria, and fungi are also beneficial for desert plants in coping with unfavourable conditions (Soussi et al., 2016; Liu et al., 2021). Nevertheless, the mechanisms underlying the development of dryland plant microbiome remain very limited, impeding our understanding of desert ecological functions and processes.

Recently, niche differentiation of plant-associated microbial taxa, mainly at the soil-root interface (rhizosphere and root endosphere), has received great research attention (Trivedi et al., 2019; Xiong et al., 2021a; Wang et al., 2022). In fact, each plant tissue (fruits, seeds, flowers, leaves, stems, and roots) and soil habitat (rhizosphere and litter) provide unique ecological niche that supports a characteristic microbial community (Gupta et al., 2021; Vandenkoornhuyse et al., 2015; Xu et al., 2021). Potentially, different microhabitats reflect different biotic (substrate and organic matter) and abiotic (temperature and water availability) conditions (Müller et al., 2016; Zheng and Gong., 2019). Compared to other humid

ecosystems, dryland ecosystems have greater differences in biotic and abiotic conditions across microhabitats (Soussi et al., 2016; Trivedi et al., 2019). However, such interactions in dryland ecosystems remain to be elucidated.

Furthermore, recent studies suggest that the formation and development of microbial communities across microhabitats are not only controlled by environmental factors but are also strongly interrelated with each other (Zheng and Gong, 2019; Bernard et al., 2021; Walsh et al., 2021). Generally, members of the microbiome are horizontally acquired from the surrounding environments where the initial and main reservoir is the soil (Cordovez et al., 2019; Xiong et al., 2021a), while others migrate vertically via parents of the host plants (Vandenkoornhuyse et al., 2015). The belowground plant compartments harbour more microbes than aboveground plant tissues (Zheng and Gong, 2019), and the rhizosphere, a 1 mm thin zone of soil that surrounds fine roots, is more enriched with microbes than the bulk soil (Philippot et al., 2013). Thus, plant-associated microbes are selectively recruited by the plants, and the plant compartment defines the composition of the microbiomes. Taxonomic and genomic analyses have shown that there are overlapping microbial communities among different plant compartments (Cordovez et al., 2019; Edwards et al., 2015). For example, although the leaves and roots of *Arabidopsis thaliana* (L.) Heynh. have specific microbiota members, they have a part of similar functional diversities (Bai et al., 2015). Whether microbial functional overlap is attributed to the migration of microorganisms among the different compartments, and whether these compartment microbiome assemblies are mainly influenced by the soil microbiome, remain to be elucidated (Turner et al., 2013; Xu et al., 2021). Therefore, clarifying the diversity, abundance, composition, and dynamics of each microhabitat is helpful for improving the understanding of plant-environment interactions (Bulgarelli et al., 2012).

In drylands, woody plants are widely revegetated and shrubs, being the frontier species, are

frequently adopted worldwide to combat desertification and to maintain sand dune stability (Zastrow, 2019). Notably, revegetation not only improve the microenvironment, but also increase plant material input to soil (Arneth et al., 2021); however, the effect of revegetation on the assembly of plant-associated and soil microbiome should be explored. In 2011, permanent plots (*Artemisia ordosica*, *Caragana korshinskii*, *Hedysarum mongolicum*, and *Salix psammophila* plantations) were established in the study site. We found that the effect of fine roots on soil organic carbon varied across the shrublands, and soil microbial diversity and composition were also significantly different (Lai et al., 2016; Liu et al., 2018; Sun et al., 2020). Therefore, a multi-plant experiment was performed in the same permanent plots. An adjacent bare sandy land, land before revegetation, served as a control in this study. We aimed to observe: (1) a drastic microbial community differentiation among the four revegetated shrubs; (2) distinct bacterial and fungal communities and compositions across different plant species and microhabitats (phylloplane, detritusphere, root rhizoplane, rhizosphere soil, and root zone soil) and the largest microbial species reservoir found in bulk soil. Consequently, we tried to identify the mechanisms involved in the assembly processes of the plant-associated microbiomes.

2. Materials and methods

2.1. Field experiment and sampling

In 2001, four desert shrub populations, which include *A. ordosica*, *C. korshinskii*, *H. mongolicum*, and *S. psammophila*, were planted on bare sandy land at the Yanchi Research Station (37° 42′31″N/107° 13′47″E, 1,530 m above sea level, shrubland details see Lai et al. 2016), located in the Mu Us Desert, Ningxia, China were used in this study. The study area was fenced to avoiding livestock grazing and anthropogenic disturbance. The long-term mean annual temperature was 8.1 °C, ranging from -8.4–22.7 °C, and the mean annual precipitation was 292 mm at this study site (Liu et al., 2018). All selected

shrubs were synchronously planted in the same field, which was characterised by sandy soil and subjected to the same management practices (Sun et al., 2020). The field experiments (four shrubland plots and one bare sandy land) were performed in August 2018 (Table S1), when the shrubs grow vigorously. For sampling, twelve 10 m × 10 m plots were randomly selected in each shrublands. The distance between plots was range from 10 m to 100 m. The leaves (matured, 15 g), detritus (twig and leaf litter, 15 g), fine roots (< 2 mm, 15 g), soil from the rhizosphere (surrounding the fine roots, 50 g) and the root zone (under the canopy, 50 g) from three healthy shrubs in each plot (samples from three shrubs were mixed and formed a pooled sample), and bulk soil (50 g) from bare sandy land were carefully collected in a single day, using disposable gloves to avoid contamination. Root and soil samples were collected from four soil profiles (40 cm × 40 cm × 40 cm) around the shrub at a distance of 0.2 – 1.0 m. Bulk soils from the same depth were randomly collected from the bare sandy land plot adjacent to other plots. Twelve samples per sample type (soil and plant) were collected for two days (10–11 August). All samples were stored separately in sealed 50-mL centrifuge tube, immediately transported to the Magigene Biotechnology Lab (Guangzhou, Guangdong Province) on dry ice within 48 h and store at –70 °C until further molecular analyses.

2.2. DNA extraction and sequencing

All frozen samples were transported on dry ice to maintain a temperature below 4 °C for DNA extraction and sequencing as soon as possible after field sampling (within a week). Visible soil debris in plant tissues (leaf, detritus, and root) were washed using distilled water. Then, approximately 1 g of crushed plant tissue and 0.5 g of soil sample were used to extract DNA using the MoBio PowerSoil® DNA Isolation Kit (MoBio Laboratories, Inc., Carlsbad, CA, USA) and DNA samples were placed randomly across plates. The concentration and purity of all extracts were measured using the NanoDrop

One (Thermo Fisher Scientific, MA, USA) and quantified again prior to polymerase chain reaction (PCR) (Agler et al., 2016).

A two-step barcoded PCR protocol was used to maximise the phylogenetic coverage of bacteria and fungi (Bai et al., 2015; Lundberg et al., 2013). Primers for the tagging the bacterial and fungal amplicons were 515F/806R (515F: 5′-GTGCCAGCMGCCGCGGTAA; 806R: 5′-GGACTACHVGGGTWTCTAAT) and ITS5-1737F/ITS2-2043R (ITS5-1737F: GGAAGTAAAAGTCGTAACAAGG; ITS2-2043R: GCTGCGTTCTTCATCGATGC), respectively, and were used in equal concentrations (Ihrmark et al., 2012; Kembel et al., 2014). After PCR amplification, the length and concentration of amplicons were detected using 1% agarose gel electrophoresis. The PCR products were purified using the EZNA® Gel Extraction Kit (Omega Bio-Tek, Doraville, USA). Sequencing libraries were generated using NEBNext® Ultra™ DNA Library Prep Kit for Illumina® (New England Biolabs, MA, USA). Illumina MiSeq sequencing was carried out on the IlluminaHiseq2500 platform (Illumina Inc., San Diego, CA, USA) using 2×250 bp.

Quality filtering of paired-end raw reads and assembly of paired-end clean reads were performed using Trimmomatic v0.33 (http://www.usadellab.org/cms/?page=trimmomatic) and FLASH v1.2.11 (https://ccb.jhu.edu/software/FLASH/), respectively (Durán et al., 2018). Raw tag quality control was analysed using Mothur V1.35.1 (http://www.mothur.org) (Schloss et al., 2009). Operational taxonomic unit (OTU) clustering, species annotation, and phylogenetic relationship construction were performed using a combination of USEARCH v10 (Caporaso et al., 2010), KRONA, GraPhlAn, QIIME v1.9.1, and R v3.6.3 software. Contaminant sequences (e.g., protista, archaea, chloroplast, mitochondrial, and viridiplantae sequences) were filtered from the data set (Edgar, 2010). Sequences were assigned to taxonomy based on a 97% sequence similarity threshold (Gunnigle et al., 2017). In total, 17, 954, 236

174 bacterial and 14, 207, 200 fungal high-quality raw reads from 252 samples. A total of 10,000 and 20,000
175 reproducible and measurable OTUs for bacteria and fungi, respectively, were included in the complete
176 datasets, and the full dataset was split into phylloplane, detritusphere, root rhizoplane, rhizosphere, root
177 zone soil, and bulk soil sub-datasets to examine the differences among the shrub species (DeSantis et al.,
178 2006). Samples from the microhabitats (i.e., leaf, detritus, root, and soil) were rarefied separately to
179 minimise sample loss (bacteria: 34528 reads; fungi: 28374 reads). All analyses conducted had six
180 replicates. All DNA-sequencing data were uploaded to the NCBI Sequence Read Archive (SRA) with
181 the accession number SRP348383.

182 *2.3. Statistical analyses*

183 All the data and Figureures were run in the R statistical software v3.6.3 (The R Foundation for
184 Statistical Computing, Vienna, Austria; http://www.r-project.org). Data normality was examined using
185 the Shapiro–Wilk rank sum test. PROC UNIVARIATE was used to test normality of distribution and
186 homogeneity of variance for residuals. To satisfy the homoscedasticity assumption, OTUs were
187 normalised using variance-stabilizing transformation. Statistical significance was determined at $\alpha = 0.05$,
188 and when necessary, *P* values for multiple comparisons were corrected using sequential Bonferroni
189 correction. The differential abundance, richness, and α-diversity across species and microhabitats
190 were identified using two-way ANOVA models (the aov R function). For each ANOVA model, multiple
191 comparisons were FDR-corrected. Significant differences between shrub species or microhabitats were
192 evaluated with the Kruskal-Willis rank sum test (kruskal.test with dunn.test in R; FDR-corrected $p <$
193 0.05). Normality of the diversity data was checked with the Shapiro-Wilk test. If the data was skewed,
194 $\log_{10}$-transformed data were used to statistical analysis. Differential abundances for bacteria and fungi in
195 each shrubland and microhabitat compared with bare sandy land were determined using DESeq2 (Love

196 et al., 2014), with FDR-corrected $p < 0.05$ considered significant.

197 To determine the differences in the microbial community, Bray-Curtis dissimilarity matrices were
198 calculated and then visualised with non-metric dimensional scaling (NMDS) ordinations. Permutational
199 multivariate analysis of variance (PERMANOVA) pairwise comparisons were conducted using the
200 adonis function in the R package vegan with 999 permutations for bacteria and fungi for statistically
201 supporting the visual clustering results of the NMDS analyses (Oksanen et al., 2019). The co-occurrence
202 network was constructed using the IGRAPH package in R, based on Spearman's rank correlations of all
203 OTUs, accompanied by the calculations of the descriptive and topological network properties (Hartman
204 et al., 2018), and visualised the significant correlations (Spearman's $r > 0.6$ or $r < –0.6$, $p < 0.01$) in
205 GEPHI v.0.9.2 (https://gephi.org/). The average degree (the number of direct correlations to a node) is
206 defined as the network complexity.

207 SourceTracker, based on Bayesian approach, was performed to evaluate the source of the plant
208 microbial communities in each habitat (Knights et al., 2011; Xiong et al., 2021b). To further support the
209 microbial source analysis, nestedness analysis was performed. The temperature statistics (*T*, smaller the
210 *T* value, perfect the nestedness), based on pairwise compositional difference, and the nestedness metric,
211 based on overlap and decreasing fill, were calculated using the R packages vegan and bipartite (Bernard
212 et al., 2021).

213 Null model and βNTI (β-nearest taxon index metrics) analyses were calculated using the picante R
214 package for distinguishing different community ecological processes, including deterministic ($|\beta NTI| >$
215 2) and stochastic process ($|\beta NTI| > 2$) (Kembel et al., 2010). Specifically, based on the βNTI and the
216 Bray-Curtis-based Raup-Crick (RC_{bray}), the two ecological processes were divided into five processes:
217 heterogeneous selection ($\beta NTI < -2$), homogeneous selection ($\beta NTI > +2$), dispersal limitation ($|\beta NTI| <$

2 and RCBray > 0.95), homogenizing dispersal (|βNTI|< 2 and RCBray < –0.95), and undominated (|βNTI|< 2 and |RCBray|< 0.95) (Tripathi et al., 2018).

3. Results

3.1. Effects of revegetated shrubs on microbial communities

A total of 48 bacterial phyla were observed in both shrub-associated and bulk soil samples. The bacterial communities were dominated by Proteobacteria, Actinobacteria, Bacteroidetes, Acidobacteria, Chloroflexi, and Planctomycetes (Figure. 1a). Notably, Cyanobacteria and Tenericutes were highly abundant in the *S. psammophila* samples. In the bare sandy land plot, Gemmatimonadetes and Planctomycetes also were the dominant bacterial phyla. Specifically, the shrub microhabitats recruited Fusobacteria, which were not detected in the bulk soil samples. At the family level, *Burkholderiaceae*, *Chitinophagaceae*, and *Sphingomonadaceae* were the top three families in the bacterial assemblage in shrub samples, while the following taxonomic ranks were dramatically different. In the fungal family, the taxonomic ranks varied markedly across shrub and bare sandy land samples. Moreover, nine fungal phyla were found in all the samples (Figure. 1b). Ascomycota was the most abundant phylum in all the samples, whereas Basidiomycota, Chytridiomycota and unclassified taxa were highly abundant in bulk soil samples. Additionally, Blastocladiomycota only was found in *C. korshinskii* and *S. psammophila* samples.

The α-diversity of bacteria and fungi (Observed species, Chao1 index, Shannon diversity index, and Goods coverage) were not significantly different across shrub plantations ($p > 0.05$; Figure. S1). However, bacterial Goods coverage in *A. ordosica* samples was lower than that in *S. psammophila* ($p < 0.01$; Figure. S1a). Beta-diversity based on average Bray-Curtis distances was markedly different across four shrub plantations and shrub species explained far greater variation in fungal community composition (Adonis:

degree of freedom (d.f.) = 3; coefficient of determination (R^2) = 0.087; $p < 0.001$) than in bacterial community composition (Adonis: d.f. = 3; $R^2 = 0.033$; $p < 0.001$; Figures. 2a and b; Table 1).

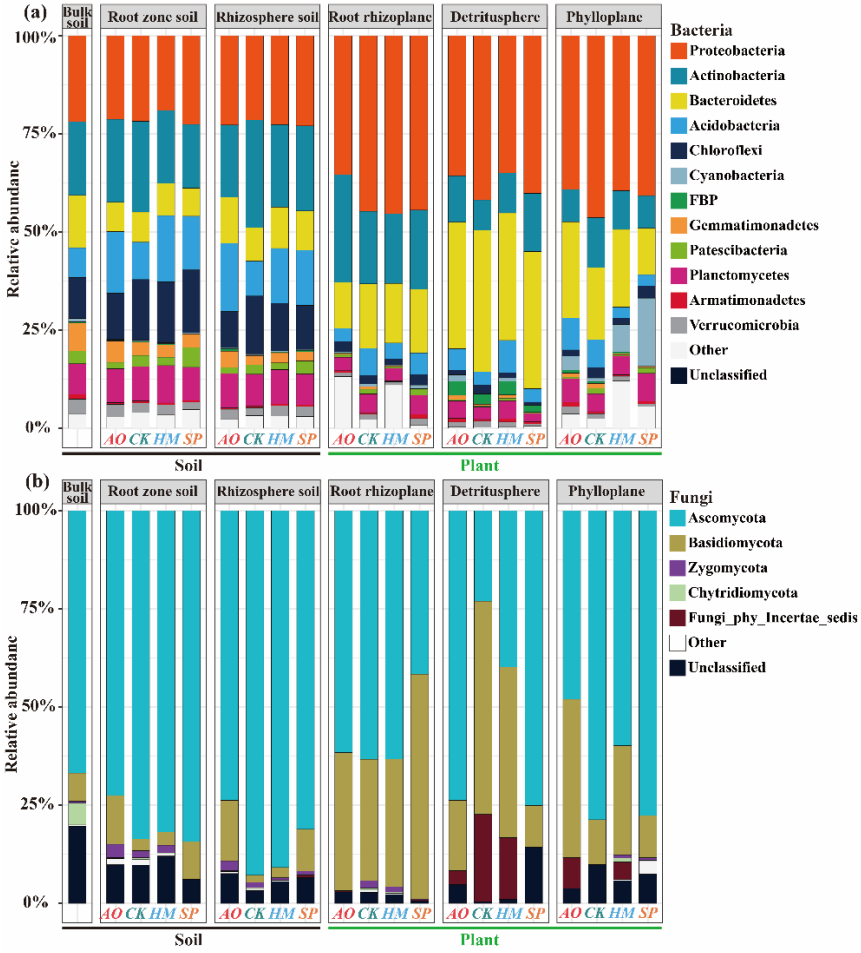

Figure 1. Relative sequence abundance of bacterial (a) and fungal (b) phyla associated with six microhabitats (bulk soil, root zone soil, rhizosphere soil, root rhizoplane, detritusphere, and phylloplane) across four shrublands (*A. ordosica*, *C. korshinskii*, *H. mongolicum*, and *S. psammophila*; n = 12) and bare sandy land (n = 12). Operational taxonomic unit with relative abundance < 0.1% were discarded.

Table 1 PERMANOVA (Bray-Curtis distance) analysis showing the ability of variables to explain compositional variance.

Domain	Variable	*df*	R^2	*P*	*Residual*
Bacteria	Host	3	0.033	**<0.001**	236
	Microhabitat	5	0.304	**<0.001**	246
	Host × Microhabitat	19	0.427	**<0.001**	220
Fungi	Host	3	0.087	**<0.001**	236
	Microhabitat	5	0.222	**<0.001**	246
	Host × Microhabitat	19	0.530	**<0.001**	220

df: degree of freedom. R^2: coefficient of determination. Significant *p*-values ($p < 0.05$) are indicated in bold texts.

252

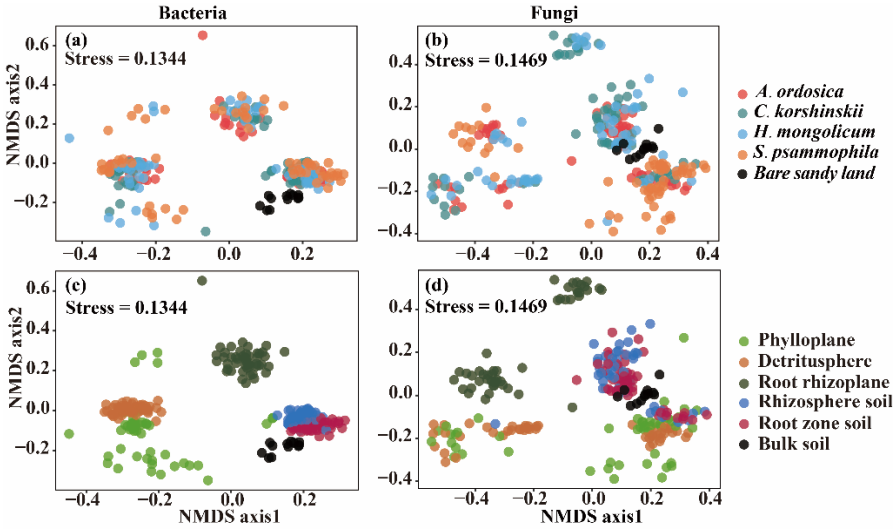

253

254 **Figure 2.** Factors shaping the composition of microbial community of xeric shrubs. (a) and (b) Non-
255 metric multidimensional scaling plots of bacterial and fungal community dissimilarity with shapes by
256 four shrub species (*A. ordosica*, *C. korshinskii*, *H. mongolicum*, and *S. psammophila*) and bare sandy
257 land. (c) and (d) Non-metric multidimensional scaling plots of bacterial and fungal community
258 dissimilarity with shapes by six microhabitats (bulk soil, root zone soil, rhizosphere soil, root rhizoplane,
259 detritusphere, and phylloplane).

260

261 The DESeq2 differential abundance analysis showed that approximate 5.1% of bacterial OTUs and
262 4.5% of fungal OTUs, mainly belonged to the bacterial families *Sphingomonadaceae* and
263 *Chitinophagaceae*, and the fungal families *Pezizomycotina_fam_Incertae_sedis* and *Trichocomaceae*,
264 respectively, were significantly enriched in four revegetated shrublands (Figure. 3; Table S2). We also
265 found that approximate 8.2% of bacterial OTUs and 4.5% of fungal OTUs significantly depleted in four
266 revegetated shrublands, these OTUs were mainly from the bacterial families *Gemmataceae* and
267 *Gemmatimonadaceae*, and the fungal family *Pezizomycotina_fam_Incertae_sedis* (Figure. 3; Table S2).
268 Specially, *S. psammophila* possessed the lowest numbers of enriched OTUs for bacteria, while *A.*

269 *ordosica* possessed the greatest numbers of enriched OTUs for fungi.

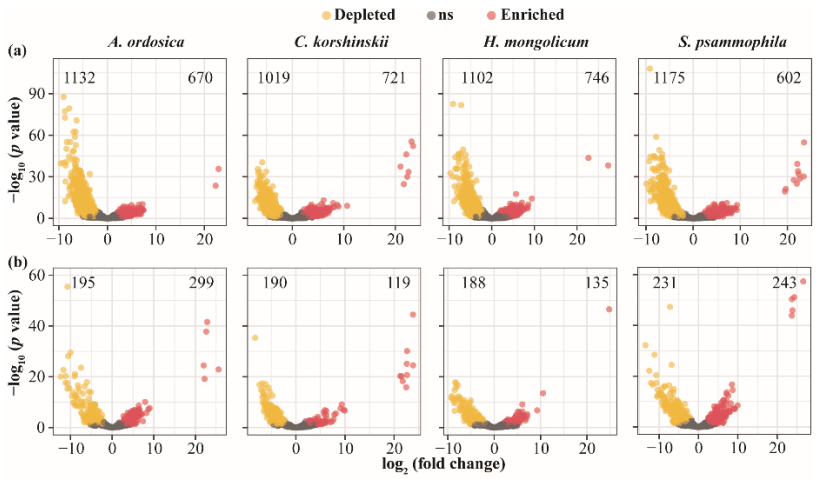

270

271 **Figure 3.** The volcano plot illustrating the enrichment and depletion patterns of the shrub-associated

272 bacterial (a) and fungal (b) communities in different revegetated shrublands (*A. ordosica*, *C. korshinskii*,

273 *H. mongolicum*, and *S. psammophila*) compared with bare sandy land.

274

275 *3.2. Niche differentiation of shrub-associated microbiota across different microhabitats*

276 The dominant bacterial and fungal phyla dramatically differed across the microhabitats (phylloplane,

277 detritusphere, root rhizoplane, rhizosphere soil, root zone soil, and bulk soil; $p < 0.01$; Figure. 1).

278 Proteobacteria and Bacteroidetes had higher abundance in plant tissue samples than soil samples, but the

279 abundance of Acidobacteria and Planctomycetes were lower in plant tissue samples ($p < 0.001$).

280 Specifically, Proteobacteria, Bacteroidetes, Actinobacteria, Acidobacteria, and Planctomycetes (average

281 across shrub species; n = 12) were abundant in all microhabitats, whereas Cyanobacteria, FBP,

282 Tenericutes, and Chloroflexi were more abundant in leaves, detritus, roots, and soils, respectively,

283 compared to other microhabitats (Tukey's honestly significant difference test: $p < 0.01$). Ascomycota and

284 Basidiomycota were the most dominant, accounting for approximately 85% of the sequences.

285 Interestingly, more fungal phyla were detected in the leaf samples than in the other samples.

Blastocladiomycota was only detected in leaf samples of *C. korshinskii* and *S. psammophila*.

The Observed species, Chao1 index, Shannon index, and Goods coverage values showed a similar trend for bacterial α-diversity among microhabitats, with a significant difference between the soil microhabitats (rhizosphere, root zone, and bulk soil) and the plant tissue microhabitats (root rhizoplane, detritusphere, and phylloplane) (Kruskal–Wallis test and Dunn's post-hoc test, $p < 0.001$; Figure. S2). Specially, in the plant tissue microhabitats, the Observed species and Shannon index of the detritusphere were significantly higher than other microhabitats ($p < 0.05$). In the soil microhabitats, the root-associated soil had greater Chao1 index than bulk soil did ($p < 0.01$). For fungi, the α-diversity index had a dramatical difference between detritusphere and other microhabitats, with a slight difference in Observed species and Shannon index (Figure. S2b).

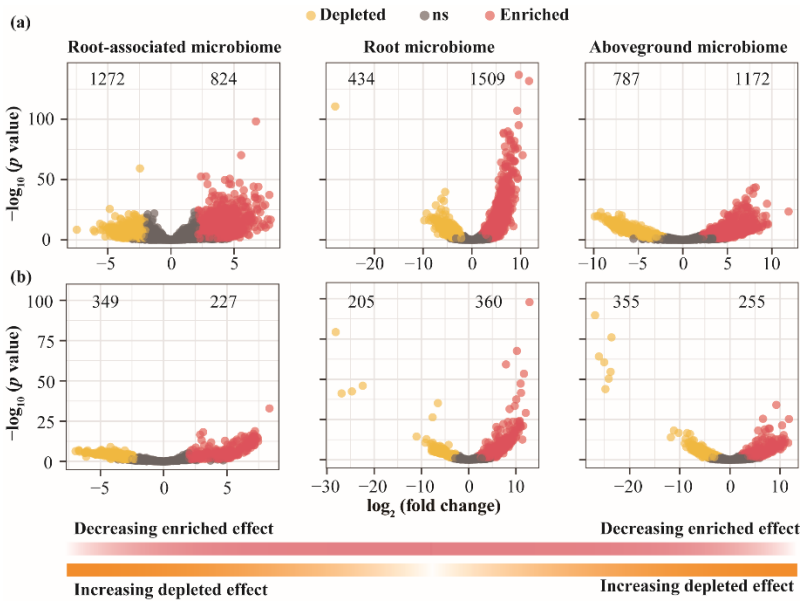

Figure 4. The volcano plot illustrating the enrichment and depletion patterns of the shrub-associated bacterial (**a**) and fungal (**b**) communities in six microhabitats (phylloplane, detritusphere, root rhizoplane, rhizosphere soil, and root zone soil) compared with bulk soil.

The differential abundance analysis demonstrated that root rhizoplane possessed the greatest numbers of enriched OTUs, mainly from the bacterial family *Gemmataceae* and the fungal family

302 *Pezizomycotina_fam_Incertae_sedis* (Figure. 4; Table S3). Meanwhile, the lowest numbers of depleted
303 OTUs, mainly belonged to the bacterial family *Chitinophagaceae* and the fungal family *Thelephoraceae*
304 was also observed in root rhizoplane (Figure. 4; Table S3). In soil microhabitats (rhizosphere and root
305 zone soil), the enriched OUTs for bacteria and fungi were mainly assigned to the families
306 *Gemmatimonadaceae* and *Gemmataceae*, and *Spizellomycetaceae* and *Lasiosphaeriaceae*, respectively.
307 Compared to soil microhabitats, the aboveground microhabitats (detritusphere and phylloplane) had the
308 greater numbers of the enriched OTUs, mainly from the bacterial families *Gemmatimonadaceae* and
309 *Pirellulaceae*, and the fungal families *Pezizomycotina_fam_Incertae_sedis* and *Trichocomaceae* (Table
310 S3).

311 Microhabitat was the primary factor explaining the variation in shrub-associated microbial
312 community composition (Adonis: d.f. = 5; bacteria: $R^2 = 0.30$; $P < 0.001$; fungi: $R^2 = 0.22$, $p < 0.001$;
313 Table 1). PERMANOVA, conducted separately for shrubs, indicated that the microbial community
314 composition significantly varied among different microhabitats (Table S4; $p < 0.01$). Community
315 similarity analysis showed that rhizosphere, root zone, and bulk soil samples were closely related to each
316 other and detritus samples were the most similar to leaf samples. In addition, root rhizoplane samples
317 were dissimilar to the other samples.

318 The network analysis showed that microbial co-occurrence patterns differed distinctly across six
319 microhabitats, particularly for the bulk soil and root rhizoplane (Figures. 5a and b, Tables S5 and S6).
320 Bacterial network in bulk soils was the most complex, followed by phylloplane and root-associated
321 microhabitats (root zone soils, root rhizoplane, and rhizosphere soils), with the lowest bacterial network
322 complexity in the detritusphere. For fungi, the highest and lowest network complexity was found in the
323 root rhizoplane and rhizosphere soils, respectively. The network complexity in bulk soils was greater

than that in other microhabitats (phylloplane > detritusphere > root zone soils), and the highest modularity and the lowest average path distance were observed in the bulk soil. We defined the "network hubs" (degree > 50; closeness centrality > 0.3) in the network, and found 1038 network hubs (bacteria: 697, fungi: 341) at bulk soil, and 157 network hubs (bacteria: 0, fungi: 157) at root rhizoplane, and 51 network hubs (bacteria: 0, fungi: 51) at detritusphere (Figure. 5c, Table S5). In the bacterial network, a half of nodes were assigned to the top 3 phyla (Proteobacteria, Planctomycetes, Actinobacteria) in soil microhabitats (bulk soil, root zone soil, rhizosphere soil), whereas in plant microhabitats (root rhizoplane, detritusphere, phylloplane) the top-three phyla were Proteobacteria, Bacteroidetes, and Actinobacteria (Figure. 5b, Table S6). For fungi, two phyla (Ascomycota and Basidiomycota) were identified in nodes, accounting for approximate 80% of all nodes. Remarkably, Zygomycota and Glomeromycota were not detected in network nodes of detritusphere (Figure. 5b, Table S6).

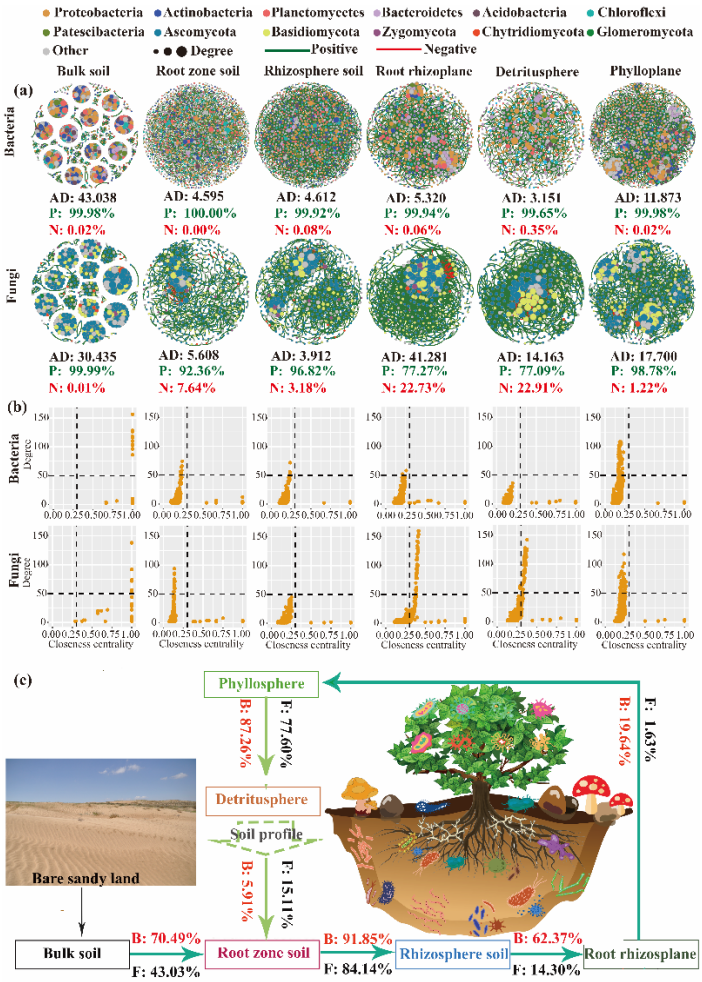

335

336 **Figure 5.** Spatial dynamics of xeric shrub-associated microbiomes. (a) Bacterial and fungal co-
337 occurrence networks along the soil-plant continuum (n = 48). AD: average degree. Different colours
338 represent microbial phyla. (b) Distribution patterns of the hub nodes (degree > 50; closeness centrality >
339 0.3) of bacterial and fungal network in different microhabitats. (c) Source model analysis based on the
340 SourceTracker showing the potential sources of xeric shrub-associated microbiota (n = 48).

341

342 *3.3. Potential sources of shrub-associated microbiota*

343 The SourceTracker analyses suggested that root-associated bacterial communities were mainly
344 derived from bulk soils and gradually transmitted to different belowground microhabitats (Figure. 5c).
345 Nevertheless, similar source patterns were not observed in root-associated fungal communities. Plant

346 tissue niches accounted for a smaller proportion of derivation of fungal communities than of bacterial
347 communities. Phylloplane, the main potential source of detritusphere, acquired a minority of taxa from
348 the belowground species pool (bacteria: 19.64%, fungi: 1.63%). Conversely, the aboveground species
349 pool was also a potential source of soil microhabitats, specifically, the detritusphere contributed 5−15%
350 of sources to the subterranean microbiotas (Figure. S5). Nestedness analysis also showed that bacterial
351 communities were more perfectly nested by habitats than fungal communities (bacteria: $T = 9.74°$, $P =$
352 0.01, NODF = 19.28%; fungi: $T = 31.38°$, $P = 0.01$, NODF = 57.61%), with rhizosphere soils having the
353 highest microbial diversity. Specifically, fungal communities in the phylloplane were an important
354 species subset.

355 *3.4. Assembly processes of shrub-associated microbiomes*

356 Null model analyses revealed that the relative importance of determinism vs. stochasticity in shrub-
357 associated bacterial and fungal communities varied across six microhabitats (Figure. 6). After quantifying
358 the deviation in βNTI values, we observed that deterministic assembly processes, especially
359 homogeneous selection, represented a predominantly higher percentage than stochastic assembly
360 processes in bacterial communities, while the stochastic assembly processes (dispersal limitation and
361 undominated processes) were dominant in fungal communities (Figure. 6). Notably, for belowground
362 habitats, the relative contribution of determinism and stochasticity showed a slightly increasing tendency
363 from bulk soil to root rhizoplane in bacterial and fungal communities, respectively (Figure. 6a).

364

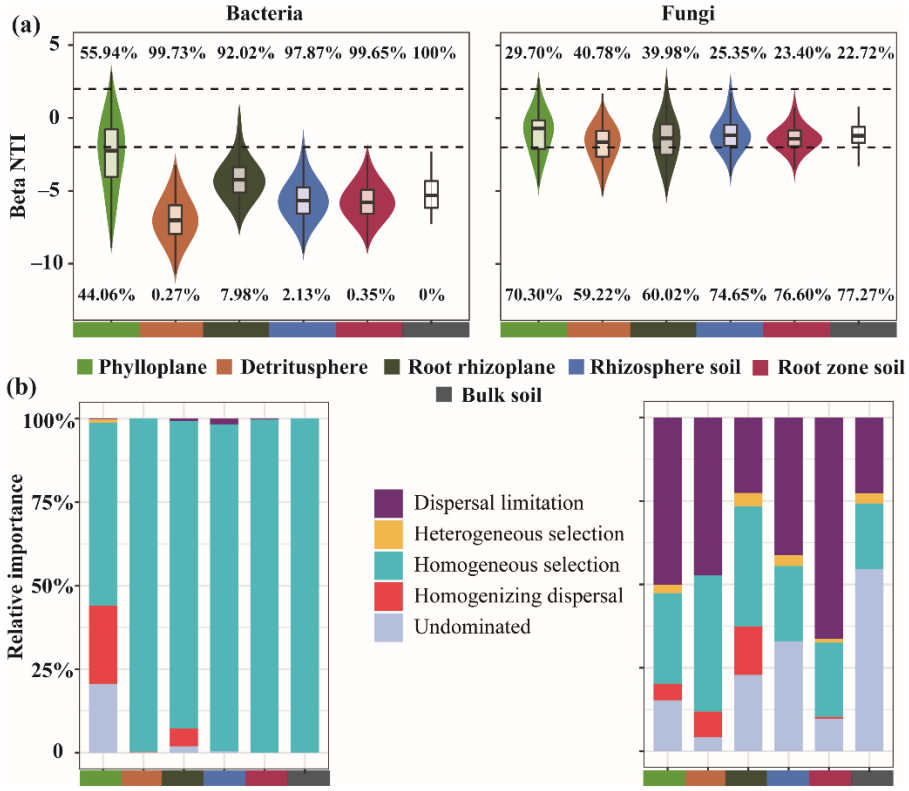

Figure 6. Bacterial and fungal community assembly processes in six microhabitats. (a) The values of the β-Nearest Taxon Index value (βNTI) for shrub-associated microbial communities. Dashed lines represent upper and lower significant thresholds at βNTI = −2 and +2, respectively. (b) The fraction of shrub-associated microbial community assembly governed principally by deterministic processes (heterogeneous selection and homogeneous selection) or stochastic processes (dispersal limitation, homogenizing dispersal, and undominated processes).

4. Discussion

4.1. Shrubs harbour different microbial communities across different microhabitats

Although the α-diversity analysis indicated that there were no dramatic differences across four shrublands, results of PERMANOVA and differential abundance analysis supported the first two hypotheses that the four revegetated shrub species recruit markedly distinct bacterial and fungal communities after colonisation on bare sandy land, with a great difference in microbial compositions across microhabitats (phylloplane, detritusphere, root rhizoplane, rhizosphere soil, and root zone soil;

379 Figures. 1–4, S1–S4). In addition, niche differentiation, rather than plant species, shaped the diversity
380 and structure of microbiomes (Table 1). Previous studies have shown that the introduction of shrubs on
381 bare sandy land changed the abundance, diversity, and composition of soil bacterial and fungal
382 communities in the degraded dryland ecosystem (Cregger et al., 2018; Sun et al., 2019), whereas our
383 results provide a more precise case assessment of the promotion of biodiversity in revegetated drylands.
384 In the results, the pattern of niche driving to microbial was supported by some studies on crops
385 (Xiong et al., 2021a, b) and wild plants (Cregger et al., 2018; Zheng and Gong, 2019; Wang et al., 2022)
386 from local to regional areas. However, recent studies have shown that fungal compositional variance is
387 better predicted by sampled sites than by microhabitats in regional areas (Bernard et al., 2021; Thiergart
388 et al., 2020). This phenomenon was confirmed in the present study site where the four shrubs encountered
389 similar growth conditions (soil and climate) but the numerous microenvironment properties (e.g.,
390 nutrients, temperature, humidity, and plant immunity) varied remarkably across the soils and plant tissues.
391 Moreover, the microbial co-occurrence network analysis indicated that the different topological
392 structures (i.e., network complexity, modularity, clustering coefficient, and hub node) between soils and
393 plant habitats influenced the bacterial communities more than the fungal communities (Figures. 1 and 5;
394 Tables S5 and S6). Another explanation may be that fungi are more easily affected by environmental
395 conditions due to the existence of some fungal communities not directly associated with a plant (Gao et
396 al., 2020). Additionally, in desert soil with low nutrients, plants supply most of the soil organic matter
397 for microbiomes, consequently resulting in a strong relationship between plants and microbes (Hu et al.,
398 2021). All these evidences suggested that, after revegetation in drylands, the recruitment and
399 domestication to soil microbiome could depend on host selection and microhabitat differentiation caused
400 by different plant species.

401 Notably, revegetated shrubs had significantly different strategies for microbiomes colonisation
402 (Figures. 1−3, S1, and S3), implying that this process majorly influences the soil health and
403 multifunctionality. Plants create several microhabitats (phylloplane, detritusphere, root rhizoplane,
404 rhizosphere) with drastic environmental conditions for colonisation of the surrounding microbiome
405 (Cordovez et al., 2019; Trivedi et al., 2020). In addition, plants also supply different litters and secretions
406 to attract microbiomes and adapt secretion components according to the environmental changes
407 (Zhalnina et al., 2018). For example, in phosphorus-limited soils, legume roots mainly secrete citric acid,
408 fumaric, malonic, succinic, and malic acids, which are favourable for Proteobacteria growth, whereas in
409 phosphorus-rich soils, there are high levels of exudates of citrate, malate, and oxalate, stimulating growth
410 of Acidobacteria (Dai et al., 2020). Volatile oil from *A. ordosica* influences the growth of desert soil
411 microalgae *Palmellococcus miniatus*, thereby, affecting the surrounding microbiomes (Yang et al., 2012).
412 Thus, the role of plant natural accessions (i.e., root exudate, root litter, leaf litter) on the microbiome
413 assembly should be intensively studied.

414 The co-occurrence network in the plantations had a lower complexity and clustering coefficient and
415 a higher average path distance than those in bare sandy land, indicating a less compact microbial
416 association in the plant compartments than in bare sandy land (Figures. 5a, b, Tables S5 and S6). Plant
417 inputs (litter and exudates) change the cross-feeding relationships of microbes (Malik et al., 2020), which
418 reduces belowground competition for organic matter (Hu et al., 2021). The encroachment of plants results
419 in changes in the microenvironment (i.e., air temperature, soil erosion, and edaphic properties), which
420 indirectly affects the microbial community and their associations (Hu et al., 2021). In contrast, in bare
421 sandy land with limited nutrition, metabolic exchange likely promotes microbial survival and assembly
422 (Leff et al., 2017). These results imply that the microbial compositions of non-plant and plant land are

largely shaped by metabolic interactions and resource competition, respectively. Although our study provides some insights into the mechanisms underlying the plant microbiomes, longitudinal experiments should be conducted (Bai et al., 2020).

In this study, the highest network complexities were found in the phylloplane and root rhizoplane, respectively for bacteria and fungi in shrublands (Figures. 5a, b; Table S5). This could be explained by intense competition for nutrition at the interface (roots and leaves) between the plant and the environment (Mommer et al., 2016; Remus-Emsermann and Schlechter, 2018). Broad ecological differences in substrate preferences, growth rates, and stress tolerance lead to distinct trajectories in bacteria and fungi during plant recovery (Sun et al., 2017). For example, fungi are generally considered as the major decomposers of recalcitrant organic matter because of their ability to produce specific enzymes (Bani et al., 2018). Additionally, mycorrhizal fungi can directly clone living plant tissues (Tedersoo et al., 2014). Hyphae filamentous fungi also provide ecological opportunities for bacteria, leading to novel host-symbiont interactions (Emmett et al., 2021; Pawlowska et al., 2018; Yuan et al., 2021). In addition, microbial spores can diffuse via attachment to motile soil bacteria (Muok et al., 2021). In summary, under harsh conditions in drylands, soil microbiomes were extraordinarily sensitive to organic matter input and microenvironment changes via revegetation. However, the response of interspecific and intraspecific interactions between microbiomes (i.e., bacteria and fungi) should have an in-depth exploration.

4.2. Source and sink of shrub-associated microbiota

Source-tracking and nestedness analysis showed that a legacy effect of the original land use on shrub-associated microbial assembly and revealed that the legacy effect of bare sandy soil on shrub -associated bacterial communities was stronger than that on shrub-associated fungal communities (Figure. 5c). However, the results partially support the source-sink hypothesis. In concordance with previous

445 studies (Amend et al., 2019; Bernard et al., 2021), rhizospheric soil, not the root zone soil or bulk soil,
446 was identified as the main species reservoir of plant-associated microbial taxa (Figure. S5), further
447 indicating that the rhizosphere act as a hotspot of plant-microbe-soil interactions. However, another study
448 found that plant bacterial communities are gradually filtered and enriched from bulk soils to plant niches
449 (Xiong et al., 2021b). This could be primarily attributed to the harsher soil conditions (low nutrients and
450 soil moisture) in the root zone and bulk soil than in the rhizosphere in the desert ecosystem. In nutrient-
451 poor soils, the rhizosphere, being a hotspot for intense plant-soil-microbe interactions, provides a more
452 pleasant habitat for different microbiomes than that of other soil zones (Mommer et al., 2016), since roots
453 can change the microhabitat environments via dead litter and bioactive exudates (Hu et al., 2018). Thus,
454 our current results, consistent with the previous investigations, show that soil microbial communities
455 under shrub canopies and between shrub canopies have no significant difference (Sun et al., 2019). These
456 results indicate that revegetated plants could prune the original soil microbial communities and modify
457 soil microbiota composition in the whole shrubland. However, future research should focus on the role
458 of shrub root traits (i.e., elongation and turnover) and soil animals (i.e., ants and nematodes) in this
459 process.

460 Interestingly, in the present study, aboveground plant species pools also contributed to the
461 belowground microbial communities, although microbial diversity of soils was higher than that of plant
462 tissue. In particular, for fungal communities, phylloplane was the second largest species pool (Figure.
463 S5b). These vertically stratified microbiota assembly patterns have also been determined in previous
464 studies in other plant species (Amend et al., 2019). Plants specifically recruit and elaborately prune a
465 small group of beneficial microbes from the soil pool during their lifetime (van der Heijden and Schlaeppi,
466 2015). A considerable part of plant microbiome diversity, which affects germination and seedling

development, may be inherited from the seed (Walsh et al., 2021). Furthermore, experimental evidence indicates that root and phyllosphere microbes are partially inherited via vertical seed transmission (Abdelfattah et al., 2021). In clonal plants, vertical transmission between plant generations occurs in a significant proportion of symbiotic bacteria and fungi (Vannier et al., 2018). Additionally, the air microbiome contributes to phyllosphere microbiota assembly (Archer et al., 2019), which further affects the soil microbiome through rainfall and eluviation. Several fungal spores can disperse onto leaves of neighbouring plants via rain splash, even when wind flow is very low (Mukherjee et al., 2021). An alternative explanation may be that exotic herbivorous insects alter the leaf microbiome through eating leaves and carrying microorganisms, thereby, affecting the soil microbial community via litter input (Humphrey and Whiteman, 2020). Overall, the horizontal and vertical transmission pathways mostly explain the origin and dispersion of microbiomes in plants. However, other mechanisms, such as the effects of leaf-derived microbiomes on the soil microbial community and the contributions of deep soil microbiomes to plant microbiota, warrant further validation.

4.3. *Ecological assembly processes of shrub-associated microbiota*

Disentangling the assembly mechanisms of plant-associated microbiomes is imperative for better understanding the role of plant in generating and maintaining microbial diversity (Trivedi et al., 2020). In this present study, quantitative analysis of assembly processes showed that bacterial and fungal communities across different microhabitats were mainly drove by determinism and stochasticity, respectively (Figure. 6a), partially in contrast to the finding of Cao et al. (2022), who detected that the stochastic processes were dominant in bacterial communities of shrublands in eastern of the Mu Us Desert. This discrepancy can be credited to the difference in precipitations. In drylands, previous studies have proven that precipitation primarily regulated microbial assembly processes, especially bacterial

communities (Jiao et al., 2021; Naidoo et al., 2022; Yang et al., 2022), because wetter habitats promote dispersal (Cermeño and Falkowski, 2009). In the current study, bacterial community assembly was dominantly governed by homogeneous selection of deterministic processes (Figure. 6b), indicating that bacteria across six microhabitats had more similar composition (Hanson et al., 2012; Su et al., 2020). Compared to bacterial communities, fungi communities at multiple microhabitats are predominantly govern by dispersal limitation (Bonito et al. 2014; Richter-Heitmann et al., 2020; Xu et al., 2021). Our results supported this view, the proportion of dispersal limitation in fungi at all microhabitats was higher than that in bacteria (Figure. 6b), suggesting that fungi are more limited by resource availability and are more sensitive to environmental changes than bacteria do.

5. Conclusions

Our results demonstrate that plant introduction has a much stronger influence on microbial α-diversity and networks in soil microhabitats than plant microhabitats, but the effect on microbial community structure was stronger in plant tissue microhabitats than in soil microhabitats. The changes due to host effect on shrub-associated microbiome composition was stronger at the niche differentiation level rather than at the plant species level in revegetated desert shrubland. We further found that plant microbiome assembly was mainly influenced by plant select and niche filter, meanwhile, revegetated plant via microenvironment changes and microbial seedbank from parent affect soil microbial composition. Furthermore, the surrounding zone of roots is a hotpot for microbial recruitments of revegetated shrubs. Determinism played a dramatically greater role in bacterial communities than fungal communities. Of the four shrubs, *A. ordosica* exhibited the highest performance in plasticity or responsiveness of microbial communities after revegetation; thus, this shrub species is the optimal choice for increasing ecosystem biodiversity in future dryland restoration. Together these results suggest that

511 the host selection (plant niches and host genetics) and soil domestication (organic matter and microbial
512 species seed input) drive microbial community composition and functions in revegetated ecosystems.
513 Collectively, these findings significantly promote our fundamental understanding of the interactions
514 between revegetated plants and microbiomes in drylands during plant introduction. In future studies, the
515 role of plant-associated microbiomes in improving soil nutrient cycle and soil-forming processes of
516 restoring ecosystems should be investigated in depth.

517 **Acknowledgments**

518 We would like to thank Dr. Chun Miao, Dr. Liang Liu, and Mr. Shijun Liu for their cooperation and
519 assistance in experimental design and field sampling, and the staff of Guangdong Magigene
520 Biotechnology Co., Ltd., Guangzhou, China for their generous support in laboratory work. We also thank
521 Prof. Manuel Delgado-Baquerizo for his constructive and valuable comments and suggestions that helped
522 us improve this article. This work was financially supported by the National Natural Science Foundation
523 of China (Grant No. 31800611 and 31870710) and the National Key Research and Development Plan
524 (No. 2022YFE0104700). Research on soil microbiomes in Yanchi Research Station is supported by the
525 Fundamental Research Funds for the Central Universities (Grant No. PTYX202122 and PTYX202123).

526 **Author contributions**

527 Zongrui Lai and Yang Yu conceived the research idea. Zongrui Lai, Yanfei Sun, Zhen Liu, Yuxuan
528 Bai, and Shugao Qin sampled in field. Zongrui Lai, Yang Yu, Lin Miao, and Yangui Qiao analysed the
529 data. Zongrui Lai and Yanfei Sun participated in the preparation of this manuscript. Zongrui Lai, Yanfei
530 Sun, and Wei Feng made the illustrations.

531 **Declaration of Competing Interest**

532 The authors declare that they have no competing financial interests or personal relationships that

533 could have appeared to influence the work reported in this paper.

534 **Data availability**

535 All RNA-seq data were uploaded to the NCBI Sequence Read Archive (SRA) with the accession
536 number SRP348383.

537 **References**

538 Abdelfattah A, Wisniewski M, Schena L, Tack A. 2021. Experimental evidence of microbial inheritance
539 in plants and transmission routes from seed to phyllosphere and root. Environmental Microbiology
540 23:2199–2214. DOI: https://doi.org/10.1111/1462-2920.15392

541 Agler MT, Ruhe J, Kroll S, Morhenn C, Kim S-T, Weigel D, Kemen EM. 2016. Microbial hub taxa link
542 host and abiotic factors to plant microbiome variation. PLoS BiolOGY 14:e1002352. DOI:
543 https://doi.org/10.1371/journal.pbio.1002352

544 Aleklett K, Rosa D, Pickles BJ, Hart MM. 2022. Community assembly and stability in the root microbiota
545 during early plant development. Frontiers in Microbiology 13: 826521.
546 https://doi.org/10.3389/fmicb.2022.826521

547 Amend AS, Cobian GM, Laruson AJ, Remple K, Tucker SJ, Poff KE, Antaky C, Boraks A, Jones CA,
548 Kuehu D, Lensing BR, Pejhanmehr M, Richardson DT, Riley PP. 2019. Phytobiomes are
549 compositionally nested from the ground up. PeerJ 27:e6609. DOI: https://doi.org/10.7717/peerj.6609

550 Archer SDJ, Lee KC, Caruso T, Maki T, Lee CK, Cary SC, Cowan DA, Maestre FT, Pointing SB. 2019.
551 Airborne microbial transport limitation to isolated Antarctic soil habitats. Nature Microbiology
552 4:925–932. DOI: https://doi.org/10.1038/s41564-019-0370-4

553 Arneth A, Olsson L, Cowie A, Erb H, Hurlbert M, Kurz WA, Mirzabaev A, Rounsevell MDA. 2021.
554 Restoring degraded lands. Annual Review of Environment and Resources 46:569–599. DOI:

555 https://doi.org/10.1146/annurev-environ-012320-054809

556 Badri DV, Zolla G, Bakker MG, Manter DK, Vivanco JM. 2013. Potential impact of soil microbiomes
557 on the leaf metabolome and on herbivore feeding behavior. New Phytologist 198:264–273. DOI:
558 https://doi.org/10.1111/nph.12124

559 Bai Y, Müller DB, Srinivas G, Garrido-Oter R, Potthoff E, Rott M, Dombrowski N, Münch PC, Spaepen
560 S, Remus-Emsermann M, Hüttel B, McHardy AC, Vorholt JA, Schulze-Lefert P. 2015. Functional
561 overlap of the *Arabidopsis* leaf and root microbiota. Nature 528:364–369. DOI:
562 https://doi.org/10.1038/nature16192

563 Bai YX, She WW, Miao L, Qin SG, Zhang YQ. 2020. Soil microbial interactions modulate the effect of
564 *Artemisia ordosica* on herbaceous species in a desert ecosystem, northern China. Soil Biology &
565 Biochemistry 150:108013. DOI: https://doi.org/10.1016/j.soilbio.2020.108013

566 Bani A, Pioli S, Ventura M, Panzacchi P, Borruso L, Tognetti R, Tonon G, Brusetti L. 2018. The role of
567 microbial community in the decomposition of leaf litter and deadwood. Applied Soil Ecology
568 126:75–84. DOI: https://doi.org/10.1016/j.apsoil.2018.02.017

569 Beckers B, De Beeck MO, Weyens N, Boerjan W, Vangronsveld J. 2017. Structural variability and niche
570 differentiation in the rhizosphere and endosphere bacterial microbiome of field-grown poplar trees.
571 Microbiome 5:1–17. DOI: https://doi.org/10.1186/s40168-017-0241-2

572 Berg A, McColl KA. 2021. No projected global drylands expansion under greenhouse warming. Nature
573 Climate Change 11:331–337. DOI: https://doi.org/10.1038/s41558-021-01007-8

574 Berg G, Grube M, Schloter M, Smalla K. 2014. Unraveling the plant microbiome: looking back and
575 future perspectives. Frontiers in Microbiology 5:148. DOI:
576 https://doi.org/10.3389/fmicb.2014.00148

577 Bernard J, Wall CB, Costantini MS, Rollins RL, Atkins ML, Cabrera FP, Cetraro ND, Feliciano ALG,
578 Greene AL, Kitamura PK, Olmedo-Velarde A, Sirimalwatt VNS, Sung HW, Thompson LPM, Vu HT,
579 Wilhite CJ, Amend AS. 2021. Plant part and a steep environmental gradient predict plant microbial
580 composition in a tropical watershed. The ISME Journal 15:999–1009. DOI:
581 https://doi.org/10.1038/s41396-020-00826-5
582 Bulgarelli D, Rott M, Schlaeppi K, Van Themaat EVL, Ahmadinejad N, Assenza F, Rauf P, Huettel B,
583 Reinhardt R, Schmelzer E, Peplies J, Gloeckner FO, Amann R, Eickhorst T, Schulze-Lefert P. 2012.
584 Revealing structure and assembly cues for *Arabidopsis* root inhabiting bacterial microbiota. Nature
585 488:91–95. DOI: https://doi.org/10.1038/nature11336
586 Caporaso JG, Kuczynski J, Stombaugh J, Bittinger K, Bushman FD, Costello EK, Fierer N, Peña AG,
587 Goodrich JK, Gordon JI, Huttley GA, Kelley ST, Knights D, Koenig JE, Ley RE, Lozupone CA,
588 McDonald D, Muegge BD, Pirrung M, Reeder J, Sevinsky JR, Turnbaugh PJ, Walters WA, Widmann
589 J, Yatsunenko T, Zaneveld J, Knight R. 2010. QIIME allows analysis of high-throughput community
590 sequencing data. Nature Methods 7:335–336. DOI: https://doi.org/10.1038/nmeth.f.303
591 Cermeño P, Falkowski PG. 2009. Controls on diatom biogeography in the ocean. Science 325:1539–
592 1541. DOI: https://doi.org/10.1126/science.1174159
593 Cordovez V, Dini-Andreote F, Carrión VJ, Raaijmakers JM. 2019. Ecology and Evolution of plant
594 microbiomes. Annual Review of Microbiology 73:69–88. DOI: https://doi.org/10.1146/annurev-
595 micro-090817-062524
596 Cregger MA, Veach AM, Yang ZK, Crouch MJ, Vilgalys R, Tuskan GA, Schadt CW. 2018. The Populus
597 holobiont: dissecting the effects of plant niches and genotype on the microbiome. Microbiome 6: 1–
598 14. DOI: https://doi.org/10.1186/s40168-018-0413-8

599 Dai ZM, Liu GF, Chen HH, Chen CR, Wang JK, Ai SY, Wei D, Li DM, Ma B, Tang CX, Brookes PC,
600 Xu JM. 2020. Long-term nutrient inputs shift soil microbial functional profiles of phosphorus cycling
601 in diverse agroecosystems. The ISME Journal 14:757–770. DOI: https://doi.org/10.1038/s41396-
602 019-0567-9
603 Delgado-Baquerizo M, Reich PB, Trivedi C, Eldridge DJ, Abades S, Alfaro FD, Bastida F, Berhe AA,
604 Cutler NA, Gallardo A, García-Velázquez L, Hart SC, Hayes PE, He JZ, Hseu ZY, Hu HW, Kirchmair
605 M, Neuhauser S, Pérez CA, Reed SC, Santos F, Sullivan BW, Trivedi P, Wang JT, Weber-Grullon L,
606 Williams MA, Singh BK. 2020. Multiple elements of soil biodiversity drive ecosystem functions
607 across biomes. Nature Ecology & Evolution 4:210–220. DOI: https://doi.org/10.1038/s41559-019-
608 1084-y
609 DeSantis TZ, Hugenholtz P, Larsen N, Rojas M, Brodie EL, Keller K, Huber T, Dalevi D, Hu P, Anderson
610 GL. 2006. Greengenes, a chimera-checked 16S rRNA gene database and workbench compatible with
611 ARB. Applied and Environmental Microbiology 72:5069–5072. DOI:
612 https://doi.org/10.1128/AEM.03006-05
613 Durán P, Thiergart T, Garrido-Oter R, Alger M, Kemen E, Schulze-Lefert P, Hacquard S. 2018. Microbial
614 interkingdom interactions in roots promote *Arabidopsis* survival. Cell 175:973–983. DOI:
615 https://doi.org/10.1016/j.cell.2018.10.020
616 Edgar RC. 2010. Search and clustering orders of magnitude faster than BLAST. Bioinformatics 26:2460–
617 2461. DOI: https://doi.org/10.1093/bioinformatics/btq461
618 Edwards J, Johnson C, Santos-Medellin C, Lurie E, Podishetty NK, Bhatnagar S, Eisen JA, Sundaresan
619 V. 2015. Structure, variation, and assembly of the root-associated microbiomes of rice. Proceedings
620 of the National Academy of Sciences of the United States of America 112:E911–E920. DOI:

https://doi.org/10.1073/pnas.1414592112

Emmett BD, Lévesque-Tremblay V, Harrison MJ. 2021. Conserved and reproducible bacterial communities associate with extraradical hyphae of arbuscular mycorrhizal fungi. The ISME Journal 15:2276–2288. DOI: https://doi.org/10.1038/s41396-021-00920-2

Gao C, Montoya L, Xu L, Madera M, Hollingsworth J, Purdom E, Singan V, Vogel J, Hutmacher RB, Dahlberg JA, Coleman-Derr D, Lemaux PG, Taylor JW. 2020. Fungal community assembly in drought-stressed sorghum shows stochasticity, selection, and universal ecological dynamics. Nature Communications 11:1–14. DOI: https://doi.org/10.1038/s41467-019-13913-9

Gunnigle E, Frossard A, Ramond JB, Guerrero L, Seely M, Cowan DA. 2017. Diel-scale temporal dynamics recorded for bacterial groups in Namib Desert soil. Scientific Reports 7:40189. DOI: https://doi.org/10.1038/srep40189

Gupta R, Elkabetz D, Leibman-Markus M, Sayas T, Schneider A, Jami E, Kleiman M, Bar M. 2021. Cytokinin drives assembly of the phyllosphere microbiome and promotes disease resistance through structural and chemical cues. The ISME Journal 16: 1–6. DOI: https://doi.org/10.1038/s41396-021-01060-3

Hanson CA, Fuhrman JA, Horner-Devine MC, Martiny JBH. 2012. Beyond biogeographic patterns: processes shaping the microbial landscape. Nature Reviews Microbiology 10:497–506. DOI: https://doi.org/10.1038/nrmicro2795

Hartman K, van der Heijden MG, Wittwer RA, Banerjee S, Walser JC, Schlaeppi K. 2018. Cropping practices manipulate abundance patterns of root and soil microbiome members paving the way to smart farming. Microbiome 6:1–14. DOI: https://doi.org/10.1186/s40168-017-0389-9

Hu LF, Robert CAM, Cadot S, Zhang X, Ye M, Li BB, Manzo D, Chervet N, Steinger T, van der Heijden

643 MGA, Schlaeppi K, Erb M. 2018. Root exudate metabolites drive plant-soil feedbacks on growth and
644 defense by shaping the rhizosphere microbiota. Nature Communications 9:1–13. DOI:
645 https://doi.org/10.1038/s41467-018-05122-7
646 Humphrey PT, Whiteman NK. 2020. Insect herbivory reshapes a native leaf microbiome. Nature Ecology
647 & Evolution 4:221–229. DOI: https://doi.org/10.1038/s41559-019-1085-x
648 Hu WG, Ran JZ, Dong LW, Du QJ, Ji MF, Yao SR, Sun Y, Gong CM, Hou QQ, Gong HY, Chen RF, Lu
649 JL, Xie SB, Wang ZQ, Huang H, Li XW, Xiong JL, Xia R, Wei MH, Zhao DM, Zhang YH, Li JH,
650 Yang HX, Wang XT, Deng Y, Sun Y, Li HL, Zhang L, Chu QP, Li XW, Aqeel M, Manan A, Akram
651 MA, Liu XH, Li R, Li F, Hou C, Liu JQ, He JS, An LZ, Bardgett RD, Schmid B, Deng JM. 2021.
652 Aridity-driven shift in biodiversity-soil multifunctionality relationships. Nature Communications
653 12:1–15. DOI: https://doi.org/10.1038/s41467-021-25641-0
654 Ihrmark K, Bödeker ITM, Cruz-Martinez K, Friberg H, Kubartova A, Schenck J, Strid Y., Stenlid J,
655 Brandström-Durling M, Clemmensen KE, Lindahl BJ. 2012. New primers to amplify the fungal ITS2
656 region-evaluation by 454-sequencing of artificial and natural communities. FEMS Microbiology
657 Ecology 82:666–677. DOI: https://doi.org/10.1111/j.1574-6941.2012.01437.x
658 Jiao S, Chen W, Wei G. 2021. Linking phylogenetic niche conservatism to soil archaeal biogeography,
659 community assembly and species coexistence. Global Ecology and Biogeography 30:1488–1501.
660 DOI: https://doi.org/10.1111/geb.13313
661 Kembel SW, Cowan PD, Helmus MR, Cornwell WK, Morlon H, Ackerly DD, Blomberg SP, Webb CO.
662 2010. Picante: R tools for integrating phylogenies and ecology. Bioinformatics 26:1463–1464. DOI:
663 https://doi.org/10.1093/bioinformatics/btq166.
664 Kembel SW, O'Connor TK, Arnold HK, Hubbell SP, Wright SJ, Green JL. 2014. Relationships between

665 phyllosphere bacterial communities and plant functional traits in a neotropical forest. Proceedings of
666 the National Academy of Sciences of the United States of America 111:13715–13720. DOI:
667 https://doi.org/10.1073/pnas.1216057111

668 Knights D, Kuczynski J, Charlson ES, Zaneveld J, Mozer MC, Collman RG, Bushman FD, Knight R,
669 Kelley ST. 2011. Bayesian community-wide culture-independent microbial source tracking. Nature
670 Methods 8:761–763. DOI: https://doi.org/10.1038/nmeth.1650

671 Lai ZR, Zhang YQ, Liu JB, Wu B, Qin SG, Fa KY. 2016. Fine-root distribution, production,
672 decomposition, and effect on soil organic carbon of three revegetation shrub species in northwest
673 China. Forest Ecology and Management 359:381–388. DOI:
674 https://doi.org/10.1016/j.foreco.2015.04.025

675 Lebeis SL, Paredes SH, Lundberg DS, Breakfield N, Gehring J, McDonald M, Malfatti S, del Rio TG,
676 Jones CD, Tringe SG, Dangl JL. 2015. Salicylic acid modulates colonization of the root microbiome
677 by specific bacterial taxa. Science 349:860–864. DOI: https://doi.org/10.1126/science.aaa8764

678 Leff JW, Lynch RC, Kane NC, Fierer N. 2017. Plant domestication and the assembly of bacterial and
679 fungal communities associated with strains of the common sunflower, *Helianthus annuus*. New
680 Phytologist 214:412–423. DOI: https://doi.org/10.1111/nph.14323

681 Liu Z, Sun YF, Zhang YQ, Feng W, Lai ZR, Fa KY, Qin SG. 2018. Metagenomic and ^{13}C tracing evidence
682 for autotrophic atmospheric carbon absorption in a semiarid desert. Soil Biology & Biochemistry
683 125:156–166. DOI: https://doi.org/10.1016/j.soilbio.2018.07.012

684 Love MI, Huber W, Anders S. 2014. Moderated estimation of fold change and dispersion for RNA-Seq
685 data with DESeq2. Genome Biology 15:550. DOI; https://doi.org/10.1186/s13059-014-0550-8.

686 Lundberg DS, Yourstone S, Mieczkowski P, Jones CD, Dangl JL. 2013. Practical innovations for high-

687 throughput amplicon sequencing. Nature Methods 10:999–1002. DOI:
688 https://doi.org/10.1038/nmeth.2634
689 Maestre FT, Benito BM, Berdugo M, Concostrina-Zubiri L, Delgado-Baquerizo M, Eldridge DJ, Guirado
690 E, Gross N, Kéfi S, Bagouse-Pingust YL, Ochoa-Hueso R, Soliveres S. 2021. Biogeography of global
691 drylands. New Phytologist 231:540–558. DOI: https://doi.org/10.1111/nph.17395
692 Maestre FT, Delgado-Baquerizo M, Jeffries TC, Eldridge DJ, Ochoa V, Gozalo B, Quero JL, García-
693 Gómez M, Gallardo A, Ulrich W, Bowker MA, Arredondo T, Barraza-Zepeda C, Bran D, Florentino
694 A, Gaitán J, Gutiérrez JR, Huber-Sannwald E, Jankju M, Mau RL, Miriti M, Naseri K, Ospina A,
695 Stavi I, Wang D, Woods NN, Yuan X, Zaady E, Singh BK. 2015. Increasing aridity reduces soil
696 microbial diversity and abundance in global drylands. Proceedings of the National Academy of
697 Sciences of the United States of America 112:15684–15689. DOI:
698 https://doi.org/10.1073/pnas.1516684112
699 Malik AA, Swenson T, Weihe C, Morrison EW, Martiny JBH, Brodie EL, Northen TR, Allison SD. 2020.
700 Drought and plant litter chemistry alter microbial gene expression and metabolite production. The
701 ISME Journal 14:2236–2247. DOI: https://doi.org/10.1038/s41396-020-0683-6
702 Mommer L, Hinsinger P, Prigent-Combaret C, Visser EJW. 2016. Advances in the rhizosphere: stretching
703 the interface of life. Plant and Soil 407:1–8. DOI: https://doi.org/10.1007/s11104-016-3040-9
704 Mukherjee R, Gruszewski HA, Bilyeu LT, Schmale III DG, Boreyko JB. 2021. Synergistic dispersal of
705 plant pathogen spores by jumping-droplet condensation and wind. Proceedings of the National
706 Academy of Sciences of the United States of America 118:e2106938118. DOI:
707 https://doi.org/10.1073/pnas.2106938118
708 Müller DB, Vogel C, Bai Y, Vorholt JA. 2016. The plant microbiota: systems-level insights and

perspectives. Annual Review of Genetics 50:211–234. DOI: https://doi.org/10.1146/annurev-genet-120215-034952

Muok AR, Claessen D, Briegel A. 2021. Microbial hitchhiking: how streptomyces spores are transported by motile soil bacteria. The ISME Journal 15:2591–2600. DOI: https://doi.org/10.1038/s41396-021-00952-8

Naidoo Y, Valverde A, Pierneef RE, Cowan DA. 2022. Differences in precipitation regime shape microbial community composition and functional potential in Namib desert soils. Microbial Ecology, 83:689–701. DOI: https://doi.org/10.1007/s00248-021-01785-w

Oksanen J, Blanchet FG, Friendly M, Kindt R, Legendre P, Oksanen MJ, Wagner H. 2019. Vegan: Community ecology package. R package version 2.5-6. DOI: https://CRAN.R-project.org/package=vegan.

Pawlowska TE, Gaspar ML, Lastovetsky OA, Mondo SJ, Real-Ramirez I, Shakya E, Bonfante P. 2018. Biology of fungi and their bacterial endosymbionts. Annual Review of Phytopathology 56:289–309. DOI: https://doi.org/10.1146/annurev-phyto-080417-045914

Philippot L, Raaijmakers JM, Lemanceau P, van der Putten WH. 2013. Going back to the roots: the microbial ecology of the rhizosphere. Nature Reviews Microbiology 11: 789–799. DOI: https://doi.org/10.1038/nrmicro3109

Remus-Emsermann MNP, Schlechter RO. 2018. Phyllosphere microbiology: at the interface between microbial individuals and the plant host. New Phytologist 218:1327–1333. DOI: https://doi.org/10.1111/nph.15054

Richter-Heitmann T, Hofner B, Krah FS, Sikorski J, Wüst PK, Bunk B, Huang S, Regan KM, Berner D, Boeddinghaus RS, Marhan S, Prati D, Kandeler E, Overmann J, Friedrich MW. 2020. Stochastic

731 dispersal rather than deterministic selection explains the spatio-temporal distribution of soil bacteria
732 in a temperate grassland. Frontiers in microbiology 11:1391. DOI:
733 https://doi.org/10.3389/fmicb.2020.01391
734 Schloss PD, Westcott SL, Ryabin T, Hall JR, Hartman M, Hollister EM, Lesniewski RA, Oakley BB,
735 Parks DH, Robinson CJ, Sahl JW, Stres B, Thallinger GG, Horn DJV, Weber CF. 2009. Introducing
736 mothur: Open-source, platform-independent, community-supported software for describing and
737 comparing microbial communities. Applied Environmental Microbiology 75:7537–7541. DOI:
738 https://doi.org/10.1128/AEM.01541-09
739 Soussi A, Ferjani R, Marasco R, Guesmi A, Cherif H, Rolli E, Mapelli F, Ouzari HI, Daffonchio D, Cherif
740 A. 2016. Plant-associated microbiomes in arid lands: diversity, ecology and biotechnological
741 potential. Plant and Soil 405:357–370. DOI: https://doi.org/10.1007/s11104-015-2650-y
742 Sun YF, Liu Z, Zhang YQ, Lai ZR, She WW, Bai YX, Feng W, Qin SG. 2020. Microbial communities
743 and their genetic repertoire mediate the decomposition of soil organic carbon pools in revegetation
744 shrublands in a desert in northern China. European Journal of Soil Science 71:93–105. DOI:
745 https://doi.org/10.1111/ejss.12824
746 Sun YF, Zhang YQ, Feng W, Qin SG, Liu Z. 2019. Revegetated shrub species recruit different soil fungal
747 assemblages in a desert ecosystem. Plant and Soil 453:81–93. DOI: https://doi.org/10.1007/s11104-
748 018-3877-1
749 Sun S, Li S, Avera BN, Strahm BD, Badgley BD. 2017. Soil bacterial and fungal communities show
750 distinct recovery patterns during forest ecosystem restoration. Applied Environmental Microbiology
751 83:e00966-17. DOI: https://doi.org/10.1128/AEM.00966-17
752 Su YG, Liu J, Zhang BC, Zhao HM, Huang G. 2020. Habitat-specific environmental factors regulate

753 spatial variability of soil bacterial communities in biocrusts across northern China's drylands. The
754 Science of the Total Environment 719:137479. DOI: https://doi.org/10.1016/j.scitotenv.2020.137479
755 Tedersoo L, Bahram M, Põlme S, Kõljalg U, Yorou NS, Wijesundera R, Ruiz LV, Vasco-Palacios AM,
756 Thu PQ, Suija A, Smith ME, Sharp C, Saluveer E, Saitta A, Rosas M, Riit T, Ratkowsky D, Pritsch K,
757 Põldmaa K, Piepenbring M, Phosri C, Peterson M, Parts K, Pärtel K, Otsing E, Nouhra E, Njouonkou
758 AL, Nilsson RH, Morgado LN, Mayor J, May TW, Majuakim L, Lodge DJ, Lee SS, Larsson K-H,
759 Kohout P, Hosaka K, Hiiesalu I, Henkel TW, Harend H, Guo LD, Greslebin A, Grelet G, Geml J, Gates
760 G, Dunstan W, Dunk C, Drenkhan R, Dearnaley J, De Kesel A, Dang T, Chen X, Buegger F, Brearley
761 FQ, Bonito G, Anslan S, Abell S, Abarenkov K. 2014. Fungal biogeography. Global diversity and
762 geography of soil fungi. Science 346:1256688. DOI: https://doi.org/10.1126/science.1256688
763 Thiergart T, Durán P, Ellis T, Vannier N, Garrido-Oter R, Kemen E, Roux F, Alonso-Blanco C, Ågren J,
764 Schulze-Lefert P, Hacquard S. 2020. Root microbiota assembly and adaptive differentiation among
765 European *Arabidopsis* populations. Nature Ecology & Evolution 4:122–131. DOI:
766 https://doi.org/10.1038/s41559-019-1063-3
767 Tripathi BM, Stegen JC, Kim M, Dong K, Adams JM, Lee YK. 2018. Soil pH mediates the balance
768 between stochastic and deterministic assembly of bacteria. The ISME Journal 12:1072–1083. DOI:
769 https://doi.org/10.1038/s41396-018-0082-4
770 Trivedi C, Reich PB, Maestre FT, Hu HW, Singh BK, Delgado-Baquerizo M. 2019. Plant-driven niche
771 differentiation of ammonia-oxidizing bacteria and archaea in global drylands. The ISME Journal
772 13:2727–2736. DOI: https://doi.org/10.1038/s41396-019-0465-1
773 Trivedi P, Leach JE, Tringe SG, Sa TM, Singh BK. 2020. Plant-microbiome interactions: from
774 community assembly to plant health. Nature Reviews Microbiology 18:607–621. DOI:

775 https://doi.org/10.1038/s41579-020-0412-1

776 Turner TR, James EK, Poole PS. 2013. The plant microbiome. Genome biology 14:1–10. DOI:
777 https://doi.org/10.1186/gb-2013-14-6-209

778 Vandenkoornhuyse P, Quaiser A, Duhamel M, Le Van A, Dufresne A. 2015. The importance of the
779 microbiome of the plant holobiont. New Phytologist 206:1196–1206. DOI:
780 https://doi.org/10.1111/nph.13312

781 van der Heijden, M.G., Schlaeppi, K., 2015. Root surface as a frontier for plant microbiome research. P.
782 Natl. Acad. Sci. USA 112, 2299–2300. https://doi.org/10.1073/pnas.1500709112

783 Vannier N, Mony C, Bittebiere AK, Michon-Coudouel S, Biget M, Vandenkoornhuyse P. 2018. A
784 microorganisms' journey between plant generations. Microbiome 6:1–11. DOI:
785 https://doi.org/10.1186/s40168-018-0459-7

786 VanWallendael A, Soltani A, Emery NC, Peixoto MM, Olsen J, Lowry DB. 2019. A molecular view of
787 plant local adaptation: incorporating stress-response networks. Annual Review of Plant Biology
788 70:559–583. DOI: https://doi.org/10.1146/annurev-arplant-050718-100114

789 Van Zelm E, Zhang YX, Testerink C. 2020. Salt tolerance mechanisms of plants. Annual Review of Plant
790 Biology 71:403–433. DOI: https://doi.org/10.1146/annurev-arplant-050718-100005

791 Walsh CM, Becker-Uncapher I, Carlson M, Fierer N. 2021. Variable influences of soil and seed-
792 associated bacterial communities on the assembly of seedling microbiomes. The ISME Journal
793 15:2748–2762. DOI: https://doi.org/10.1038/s41396-021-00967-1

794 Wang ZY, Wang HL, Chen ZF, Wu QZ, Huang KT, Ke Q, Zhu LY, Lu S, Tang YB, Li H, Chen LJ, Wu
795 LC. 2022. Ecological niche differences regulate the assembly of bacterial community in endophytic
796 and rhizosphere of *Eucalyptus*. Forest Ecology and Management 524:120521. DOI:

https://doi.org/10.1016/j.foreco.2022.120521

Xiong C, Zhu YG, Wang JT, Singh B, Han LL, Shen JP, Li PP, Wang GB, Wu CF, Ge AH, Zhang LM, He JZ. 2021a. Host selection shapes crop microbiome assembly and network complexity. New Phytologist 229:1091–1104. DOI: https://doi.org/10.1111/nph.16890

Xiong C, Singh BK, He JZ, Han YL, Li PP, Wan LH, Meng GZ, Liu SY, Wang JT, Wu CF, Ge AH, Zhang LM. 2021b. Plant developmental stage drives the differentiation in ecological role of plant bacterial and fungal microbiomes. Microbiome 9:1–15. DOI: https://doi.org/10.1186/s40168-021-01118-6

Xu A, Liu J, Guo Z, Wang C, Pan K, Zhang F, Pan X. 2021. Distinct assembly processes and determinants of soil microbial communities between farmland and grassland in arid and semiarid areas. Applied and Environmental Microbiology 87:e01010-21. DOI: https://doi.org/10.1128/AEM.01010-21

Xu L, Pierroz G, Wipf HM-L, Gao C, Taylor JW, Lemaux PG, Coleman-Derr D. 2021. Holo-omics for deciphering plant-microbiome interactions. Microbiome 9:1–11. DOI: https://doi.org/10.1186/s40168-021-01014-z

Yang L, Ning D, Yang Y, He N, Li X, Cornell CR, Bates CT, Filimonenko E, Kuzyakov Y, Zhou JZ, Yu GR, Tian J. 2022. Precipitation balances deterministic and stochastic processes of bacterial community assembly in grassland soils. Soil Biology and Biochemistry 168:108635. DOI: https://doi.org/10.1016/j.soilbio.2022.108635

Yang XL, Deng SQ, De Philippis R, Chen LZ, Hu CZ. 2012. Chemical composition of volatile oil from *Artemisia ordosica* and its allelopathic effects on desert soil microalgae, *Palmellococcus miniatus*. Plant Physiology and Biochemistry 51:153–158. DOI: https://doi.org/10.1016/j.plaphy.2011.10.019

Yuan MTM, Kakouridis A, Starr E, Nguyen N, Shi SJ, Pett-Ridge J, Nuccio E, Zhou JZ, Firestone M. 2021. Fungal-bacterial cooccurrence patterns differ between arbuscular mycorrhizal fungi and

819 nonmycorrhizal fungi across soil niches. mBio 12:e03509-20. DOI:
820 https://doi.org/10.1128/mBio.03509-20

821 Zastrow M. 2019. China's tree-planting drive could falter in a warming world. Nature 573:474–547. DOI:
822 https://doi.org/10.1038/d41586-019-02789-w

823 Zhalnina K, Louie KB, Hao Z, Mansoori N, da Rocha UN, Shi SJ, Cho H, Karaoz U, Loqué D, Bowen
824 BP, Firestone MK, Northen TR, Brodie EL. 2018. Dynamic root exudate chemistry and microbial
825 substrate preferences drive patterns in rhizosphere microbial community assembly. Nature
826 Microbiology 3:470–480. DOI: https://doi.org/10.1038/s41564-018-0129-3

827 Zheng Y, Gong X. 2019. Niche differentiation rather than biogeography shapes the diversity and
828 composition of microbiome of *Cycas panzhihuaensis*. Microbiome 7:1–19. DOI:
829 https://doi.org/10.1186/s40168-019-0770-y

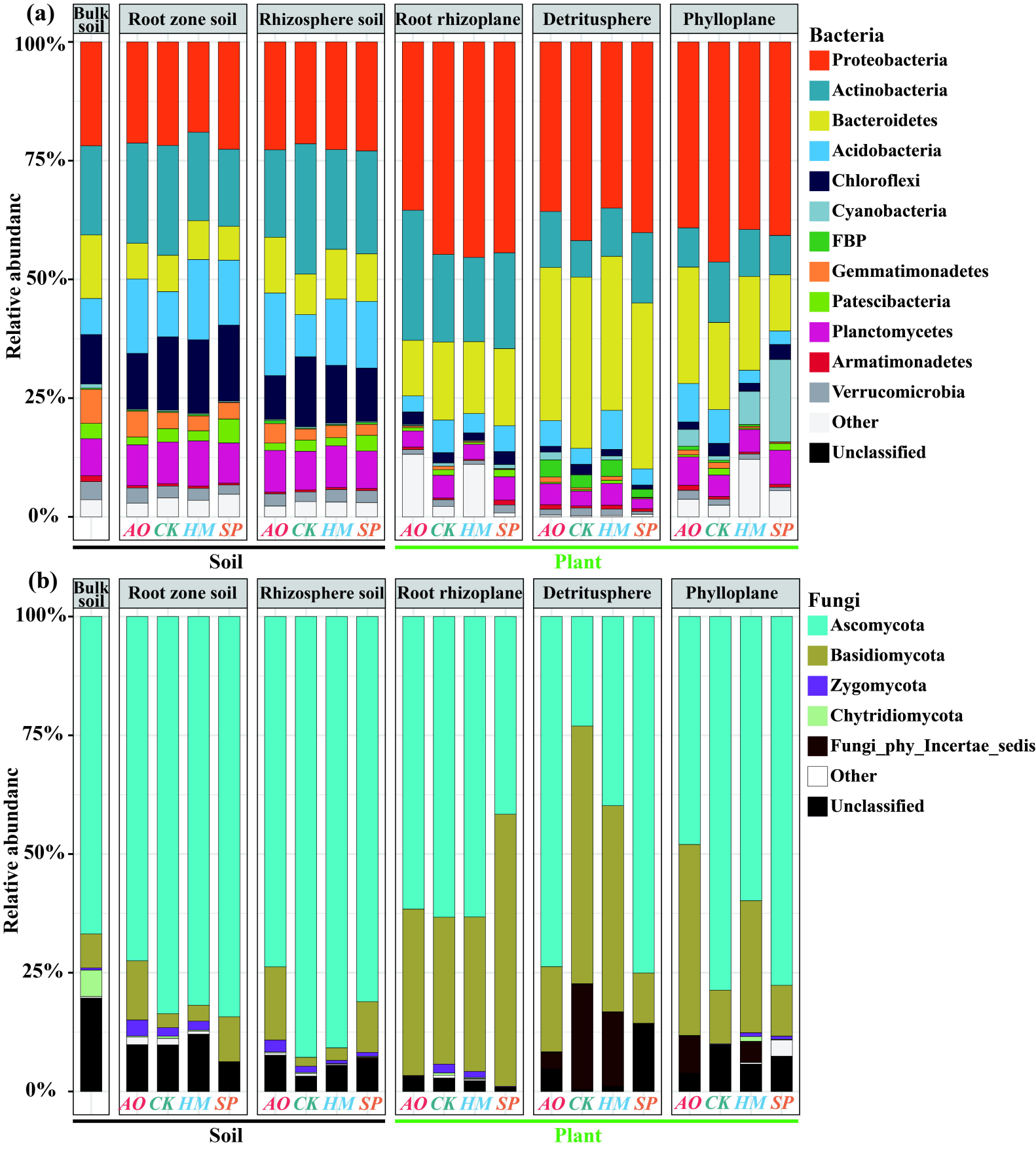
(a)
Bulk soil
Root zone soil
Rhizosphere soil
Root rhizoplane
Detritusphere
Phylloplane
100%
75%
50%
25%
0%
Relative abundanc
AO CK HM SP
Soil
Plant
Bacteria
Proteobacteria
Actinobacteria
Bacteroidetes
Acidobacteria
Chloroflexi
Cyanobacteria
FBP
Gemmatimonadetes
Patescibacteria
Planctomycetes
Armatimonadetes
Verrucomicrobia
Other
Unclassified
(b)
Fungi
Ascomycota
Basidiomycota
Zygomycota
Chytridiomycota
Fungi_phy_Incertae_sedis
Other
Unclassified

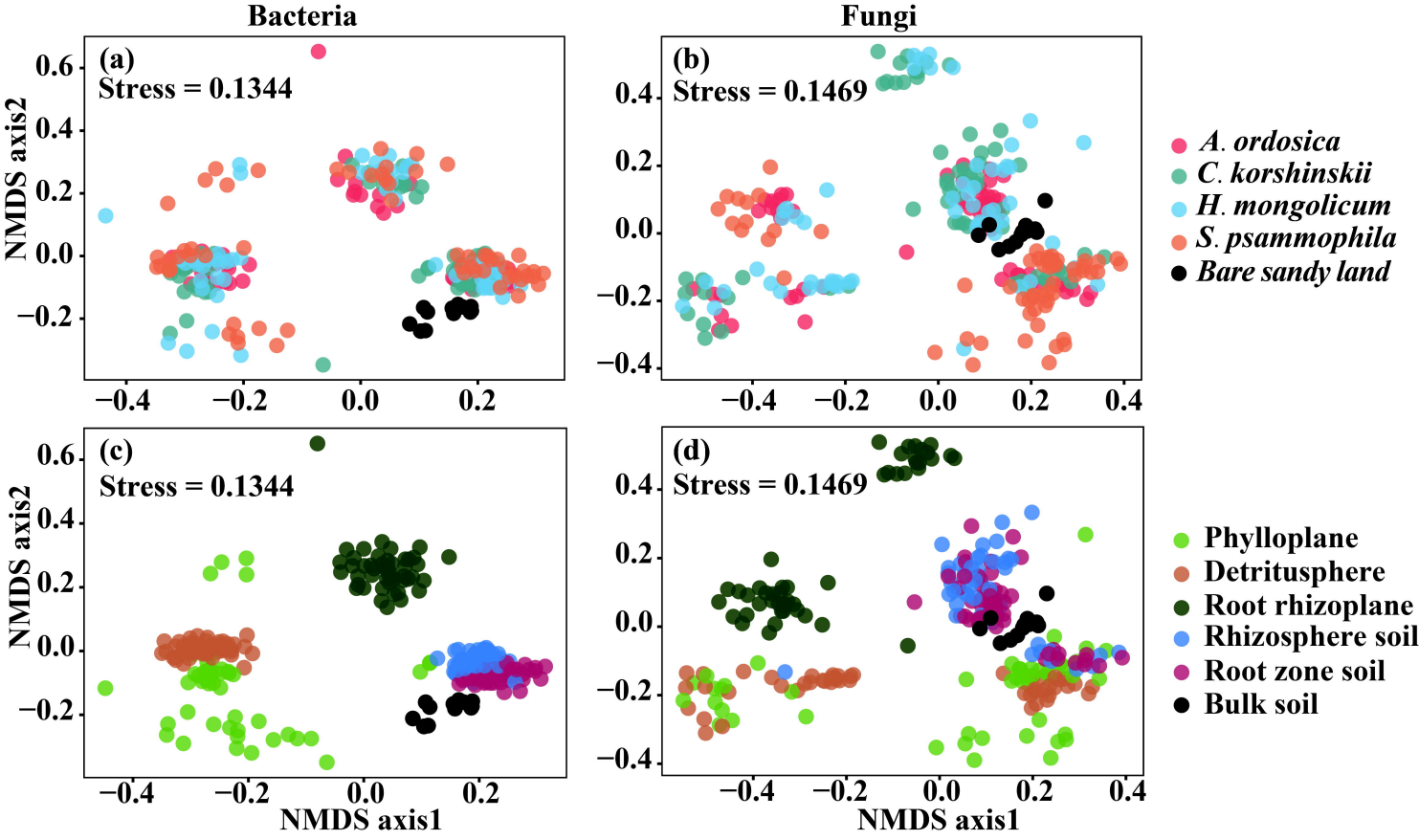
Bacteria
Fungi
(a)
Stress = 0.1344
(b)
Stress = 0.1469
(c)
Stress = 0.1344
(d)
Stress = 0.1469
NMDS axis2
NMDS axis1
A. ordosica
C. korshinskii
H. mongolicum
S. psammophila
Bare sandy land
Phylloplane
Detritusphere
Root rhizoplane
Rhizosphere soil
Root zone soil
Bulk soil

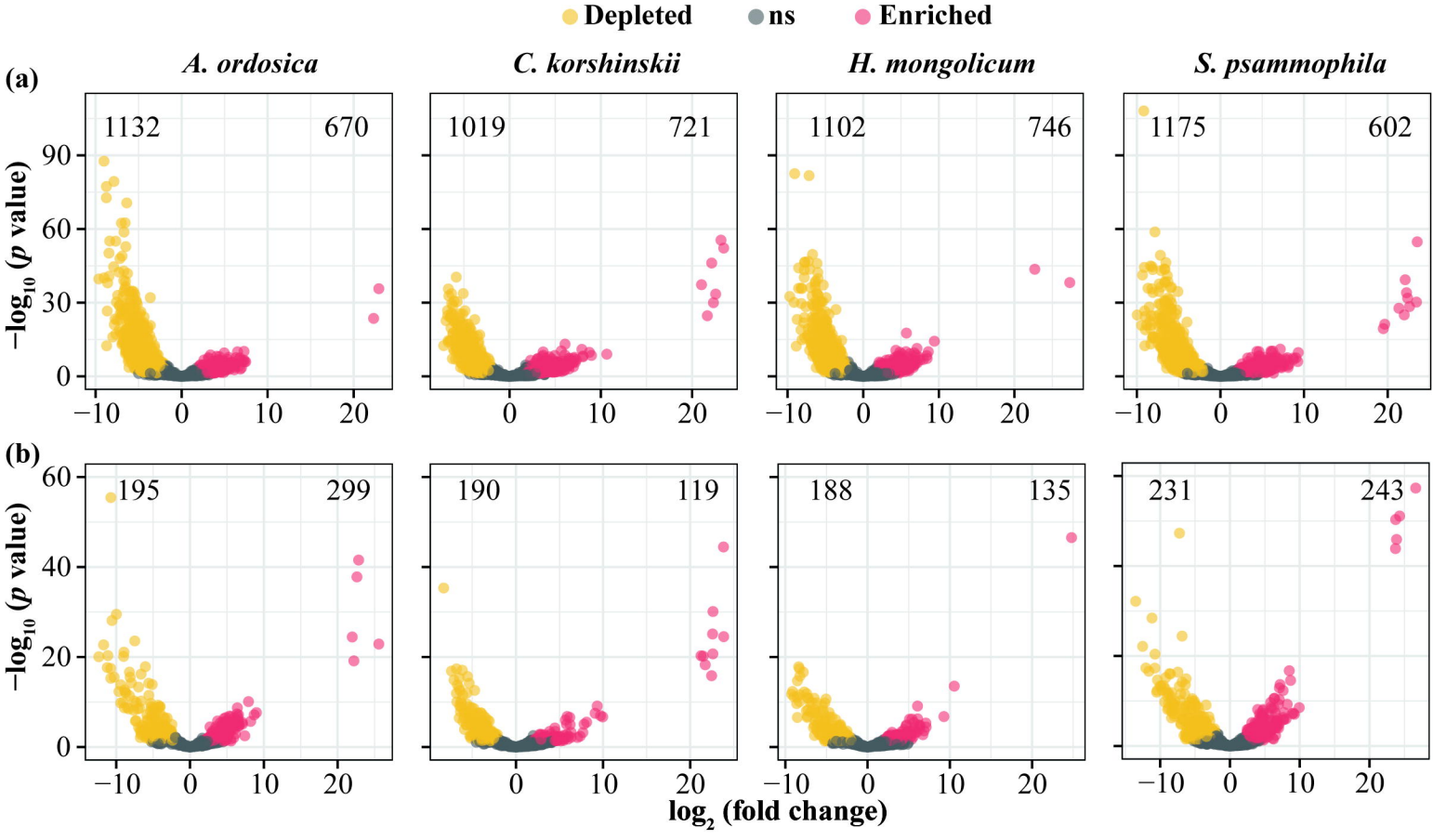
Depleted
ns
Enriched
A. ordosica
C. korshinskii
H. mongolicum
S. psammophila
(a)
(b)
1132
670
1019
721
1102
746
1175
602
195
299
190
119
188
135
231
243
−log10 (p value)
log2 (fold change)

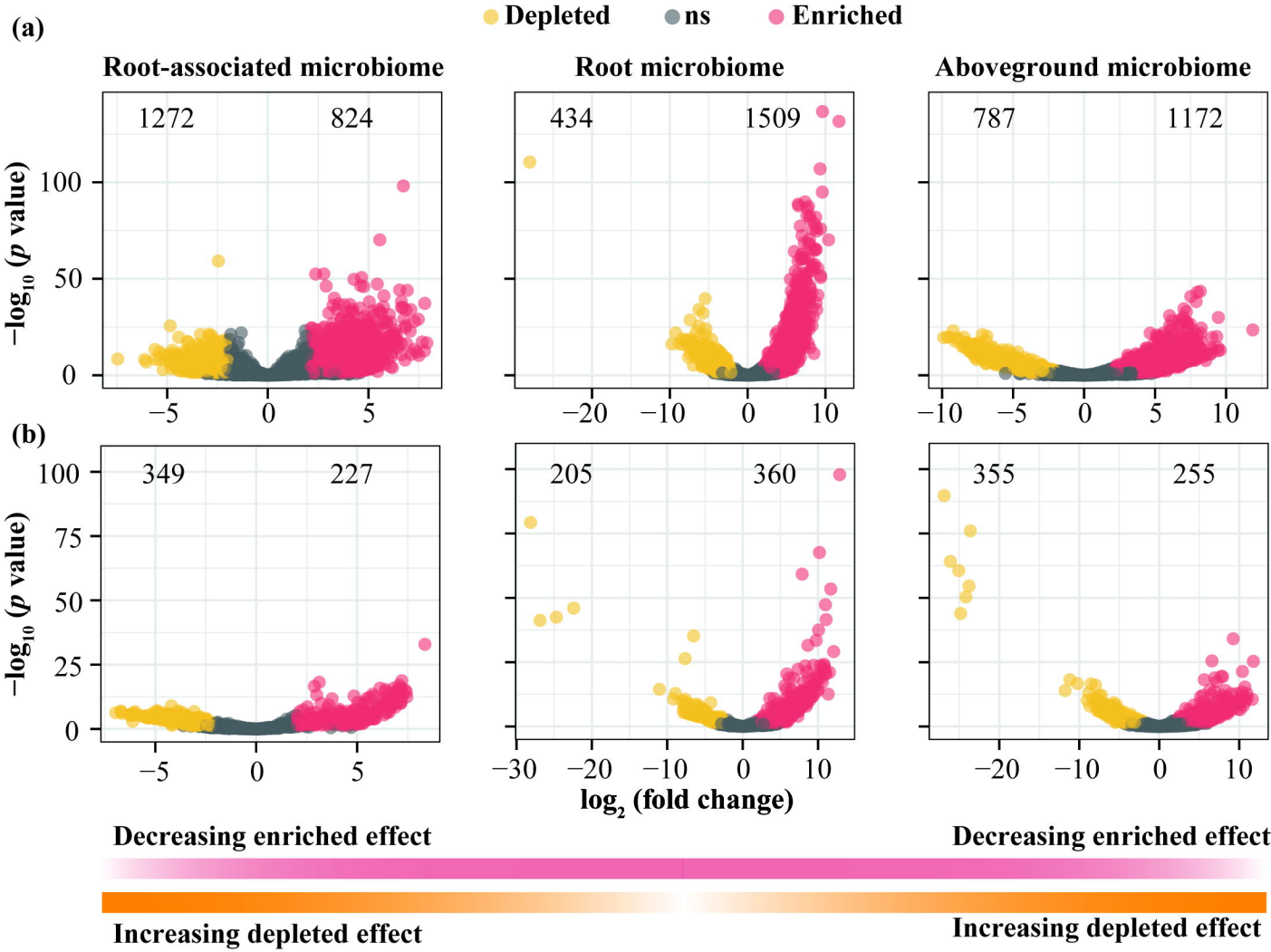
(a)
Depleted
ns
Enriched
Root-associated microbiome
Root microbiome
Aboveground microbiome
1272
824
434
1509
787
1172
−log10 (p value)
100
50
0
−5
0
5
−20
−10
0
10
−10
−5
0
5
10
(b)
349
227
205
360
355
255
100
75
50
25
0
−5
0
5
−30
−20
−10
0
10
−20
−10
0
10
log2 (fold change)
Decreasing enriched effect
Decreasing enriched effect
Increasing depleted effect
Increasing depleted effect

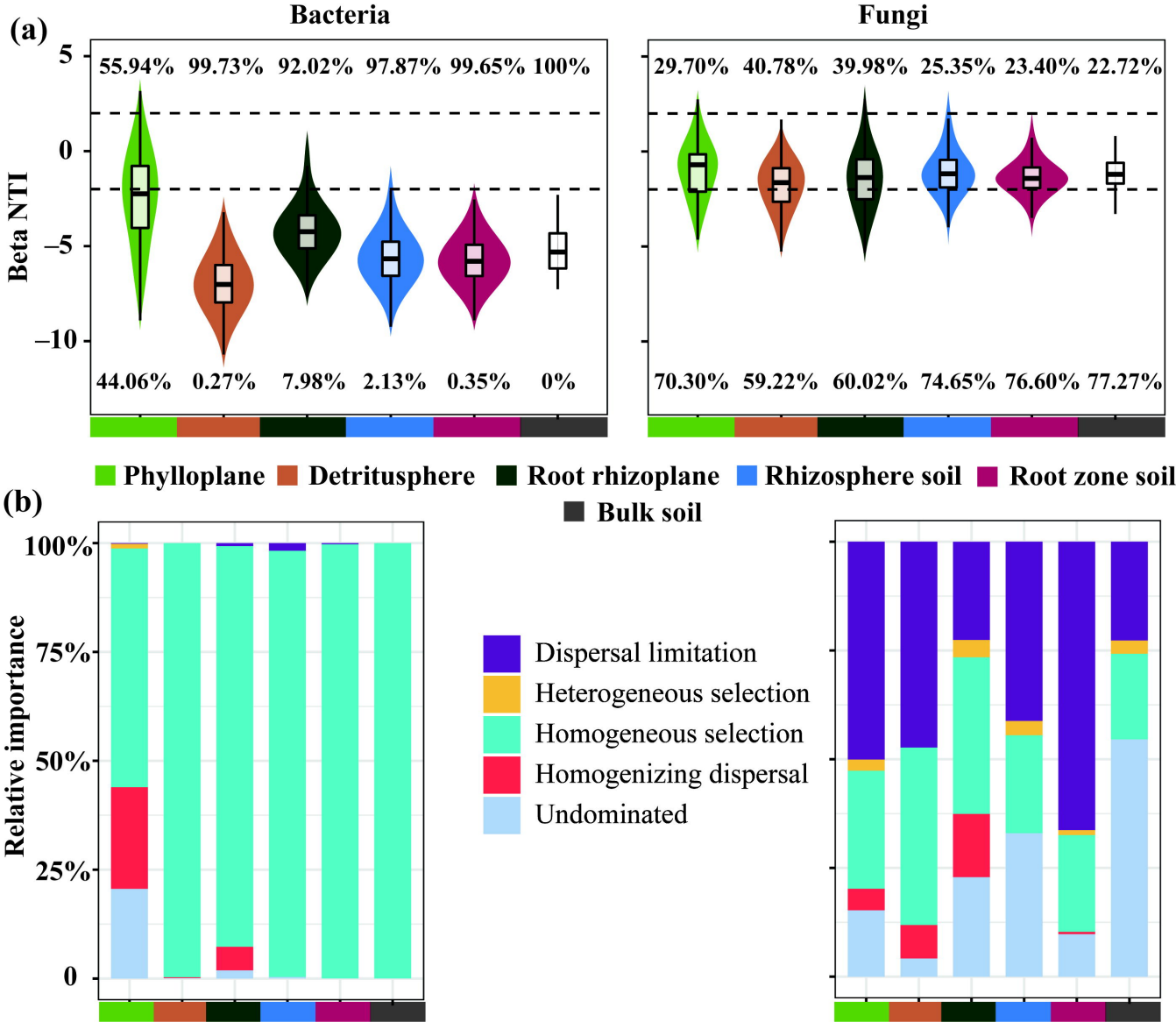
(a)
Bacteria
Fungi
Beta NTI
5
0
−5
−10
55.94%
99.73%
92.02%
97.87%
99.65%
100%
44.06%
0.27%
7.98%
2.13%
0.35%
0%
29.70%
40.78%
39.98%
25.35%
23.40%
22.72%
70.30%
59.22%
60.02%
74.65%
76.60%
77.27%
Phylloplane
Detritusphere
Root rhizoplane
Rhizosphere soil
Root zone soil
Bulk soil
(b)
Relative importance
100%
75%
50%
25%
0
Dispersal limitation
Heterogeneous selection
Homogeneous selection
Homogenizing dispersal
Undominated